

Ion screening effects and stellar collapse

S. W. Bruenn

Department of Physics, Florida Atlantic University, Boca Raton, Florida 33431-0991

A. Mezzacappa

Theoretical and Computational Physics Group, Oak Ridge National Laboratory, Oak Ridge, Tennessee 37831-6354

(Received 16 May 1997)

During the collapse of a massive star's stellar core Coulomb effects maintain the ions in a highly correlated state. This has an important consequence: Neutrino-nucleus elastic scattering, which dominates the neutrino opacity, is substantially reduced for low-energy neutrinos. This results from phase interference effects that occur when the neutrino wavelength becomes larger than the interion spacing, and is analogous to a crystal becoming transparent to x rays when the change in wave number from scattering is smaller than the reciprocal lattice spacing. This reduction in the neutrino-nucleus elastic scattering cross section, referred to as "ion screening," has been calculated most recently by Horowitz. Using his correction, we investigate its effect on stellar core collapse. Our numerical results show that ν_e downscattering with electrons is sufficiently rapid to fill the low-energy neutrino window created by ion screening, but the window width is insufficient for ion screening to have a significant effect on core deleptonization. In particular, inclusion of ion screening lowers the trapped lepton fraction by only 0.015 in both our $15M_\odot$ and a $25M_\odot$ models. We confirm this with an analytic model that elucidates ion screening's essential effect. For the sake of comparison, we also investigate the effect on core deleptonization of turning neutrino-nucleus elastic scattering off completely, and of turning off all semileptonic neutral-current neutrino scattering. These latter neutrino opacity modifications have substantially greater effects on core deleptonization than the ion-screening correction. [S0556-2821(97)06922-1]

PACS number(s): 97.60.Bw, 13.15.+g

I. INTRODUCTION

The destabilization and collapse of the core of an evolved massive star initiates a complex and incompletely understood chain of events that leads in some cases to the violent expulsion of its mantle and envelope in a supernova explosion, and the rapid evolution of the remnant core to a neutron star or a black hole (see Bethe [1] for a review, and Bruenn [2], Herant *et al.* [3], Burrows, Hayes, and Fryxell [4], Janka and Müller [5], and Mezzacappa *et al.* [6] for more recent summaries). The outwardly propagating shock ("bounce shock") launched at core rebound and perhaps rejuvenated during a reheating episode ultimately generates the explosion, if one occurs. However, the strength of the shock at formation, and therefore much of the postshock core structure and dynamics, is governed by the core hydrodynamics during infall, which is a sensitive function of the pressure deficit [7], i.e., the difference between the actual pressure and the pressure required for hydrostatic equilibrium. Because the pressure during infall is dominated by leptons (e.g., electrons, and to a lesser extent ν_e 's) until nuclear matter densities are reached, the pressure deficit is determined by the evolution of the lepton sea, viz., (1) the conversion during infall of the lepton sea from an initial composition of pure electrons to an equilibrium mixture of electrons and ν_e 's, and (2) the loss of leptons from the core by the escape of ν_e 's ("deleptonization"). While the former is generic to core collapse, the latter is a function of the neutrino opacities, or more specifically, the neutrino interaction cross sections on the various constituents of the core material, and a function of the equation of state, which determines the abun-

dance distribution of the constituent electrons, protons, neutrons, nuclei, etc.

As a result of the steady decrease in the core entropy during its thermonuclear evolution [8], it is relatively cold at destabilization—the dimensionless entropy per baryon, $s = S/n_B k$, is of order unity. (S and n_B are the entropy and baryon number per unit volume, respectively, and k is the Boltzmann constant.) This has the consequence that most of the core material is in the form of heavy nuclei. The presence of heavy nuclei and the dearth of free nucleons results in the isoenergetic coherent scattering of ν_e 's on nuclei (NAS) being the dominant neutrino opacity source, exceeding the next most important sources [ν_e -neutron and ν_e -electron elastic scattering (NES)] by between one and two orders of magnitude. (An exception to this occurs at low ν_e energies and high densities, where NES (neutrino-electron scattering) can become comparable to NAS (neutrino-nucleus isoenergetic scattering) because of the high rate of ν_e "in" scattering from higher energies. See below.) Table I summarizes the relative magnitudes of the dominant opacity sources for most conditions during core infall. The expressions for the inverse mean free paths are taken from Bruenn [9], except for ν_e -electron scattering, which is taken from Tubbs and Schramm [10]. The ratios are calculated using thermodynamic conditions ($s=1.2$, $Y_e=0.33$) typical of the infalling core material at $\rho \approx 10^{12}$ g cm $^{-3}$. (We mention that $\bar{\nu}_e$'s, ν_μ 's, $\bar{\nu}_\mu$'s, ν_τ 's, and $\bar{\nu}_\tau$'s are suppressed during infall, and only appear after the matter in the outer core has been substantially heated by the bounce shock [11,12,9].)

The large ν_e opacity provided by NAS has a profound effect on the evolution of the infalling core. At densities of about 10^{12} g cm $^{-3}$, the ν_e mean free paths become short in

TABLE I. Comparison of inverse mean free paths. Inverse mean free path ratios are computed for $\rho = 10^{12} \text{ g cm}^{-3}$, $s = 1.2$, and $Y_e = 0.33$. ϵ is the neutrino energy (MeV). G^2 is the effective weak interaction constant, which is equal to $5.18 \times 10^{-44} \text{ MeV}^{-2} \text{ cm}^2$. $\sin^2 \theta_W = 0.23$ (θ_W is the Weinberg angle). g_V is the vector coupling constant, which is equal to 1, g_A is the axial vector coupling constant, which is equal to 1.21. n_i is the number density of particles of type i (n , neutrons; p , protons; He, helium nuclei; A , heavy nuclei; e , electrons). E_e is the electron energy, $F(E_e)$ electron occupancy. E_F is the electron Fermi energy.

Inverse mean free path	Ratio
$\lambda_{\nu+A \rightarrow \nu+A}^{-1} \approx \frac{G^2}{2\pi} \epsilon^2 n_A A^2 \sin^4 \theta_W$	
$\lambda_{\nu+n \rightarrow \nu+n}^{-1} \approx \frac{G^2}{\pi} \epsilon^2 n_n \frac{1}{4} [g_V^2 + 3g_A^2]$	$\frac{\lambda_{\nu+n \rightarrow \nu+n}^{-1}}{\lambda_{\nu+A \rightarrow \nu+A}^{-1}} \sim 0.03$
$\lambda_{\nu+p \rightarrow \nu+p}^{-1} \approx \frac{G^2}{\pi} \epsilon^2 n_p \frac{1}{4} [(g_V - 2 \sin^2 \theta_W)^2 + 3g_A^2]$	$\frac{\lambda_{\nu+p \rightarrow \nu+p}^{-1}}{\lambda_{\nu+A \rightarrow \nu+A}^{-1}} \sim 0.0005$
$\lambda_{\nu+\text{He} \rightarrow \nu+\text{He}}^{-1} \approx 16 \frac{G^2}{2\pi} \epsilon^2 n_{\text{He}} \sin^4 \theta_W$	$\frac{\lambda_{\nu+\text{He} \rightarrow \nu+\text{He}}^{-1}}{\lambda_{\nu+A \rightarrow \nu+A}^{-1}} \sim 0.0001$
$\lambda_{\nu+n \rightarrow e^-+p}^{-1} \approx \frac{G^2}{\pi} \epsilon^2 n_n (g_V^2 + 3g_A^2) [1 - F(E_e)]$	$\frac{\lambda_{\nu+n \rightarrow e^-+p}^{-1}}{\lambda_{\nu+A \rightarrow \nu+A}^{-1}} \sim 0.0002$
$\lambda_{\nu+e^- \rightarrow \nu+e^-}^{-1} \approx \frac{G^2}{128\pi m_e^2 c^4} \epsilon^2 n_e \frac{\epsilon}{E_F} [(1 + 2 \sin^2 \theta_W)^2 + (2 \sin^2 \theta_W)^2]$	$\frac{\lambda_{\nu+e^- \rightarrow \nu+e^-}^{-1}}{\lambda_{\nu+A \rightarrow \nu+A}^{-1}} \sim 0.025$

comparison with the core scale height [9], effectively trapping the ν_e 's in the core for the remainder of core infall [13–16]. This limits the drop in the lepton fraction Y_l (number of leptons per baryon) from its initial value ~ 0.46 , characteristic of iron, to ~ 0.33 [9]. A value ~ 0.18 would result without the opacity contributions from neutral currents, and a value ~ 0.02 would obtain if the core contrived to remain transparent to ν_e 's throughout its collapse. Also limited by the small extent of core deleptonization is the inevitable generation of entropy that accompanies core deleptonization. The entropy generation arises from the steep energy dependence of both the electron capture rates and the neutrino opacities, which favor the capture of high-energy electrons and the escape from the core of low-energy ν_e 's, with the energy difference heating the matter. The result: The core remains relatively cold during infall, and nuclei persist until they merge to form nuclear matter at a transition density $\rho_{\text{tr}} \sim 10^{14} \text{ g cm}^{-3}$ (Bethe *et al.* [17]). The consistency of this scenario for core infall is assured by the continued presence of nuclei, which guarantees that NAS remains the dominant ν_e opacity source, and therefore that the opacity remains high.

Because NAS involves ν_e scattering from constituents (nucleons) with no change in the nucleon quantum states, the superposition principle applies, *viz.*, the resulting amplitude is a sum over constituent amplitudes. (If the nucleon quantum states are not changed, scattering on one nucleon is indistinguishable from scattering on another, and according to basic quantum mechanics, the amplitudes for the two possibilities add and interfere.) When these constituent amplitudes are all in phase, the cross section, which goes as the square of the amplitude, becomes large [18]. The magnitude of the NAS cross section, $\sigma_{\nu+A}$, and its dominance during core

infall results from this application of the superposition principle.

If $\sigma_{\nu+A}^0$ is the cross section that results when the amplitudes for scattering from the constituent nucleons of a nucleus are simply added up in phase, several important corrections must be taken into account. They may be considered in the static limit, *i.e.*, the limit of zero neutrino-energy transfer to the nuclei (see the Appendix for details). [Because $\epsilon \ll M_{\text{nuc}} c^2$ (ϵ is the ν_e energy and M_{nuc} is the nuclear mass), the energy transfer between the ν_e and the nucleus is very small.] The first correction arises when the correct phase relationships of the amplitudes for scattering from the constituent nucleons in the nucleus are taken into account, and results in a multiplicative correction referred to as the ‘‘nuclear structure function’’ or ‘‘nuclear form factor.’’ At high neutrino energies (*i.e.*, neutrino energies for which $\lambda_{\nu} < R_{\text{nuc}}$, where λ_{ν} and R_{nuc} are the ν_e wavelength and the nuclear radius, respectively), the nuclear form factor reduces $\sigma_{\nu+A}$ substantially below $\sigma_{\nu+A}^0$ because of destructive interference [18,19,20]. This correction has been routinely applied to $\sigma_{\nu+A}^0$ in supernova simulations. We will refer to the NAS cross section incorporating the nuclear form factor as $\sigma_{\nu+A}^1$.

The second correction to $\sigma_{\nu+A}^0$ has not been routinely applied in supernova simulations, and arises when the summation over amplitudes is extended to other nuclei (ions). This again results in a multiplicative correction, which is referred to as the ‘‘liquid structure function’’ or the ‘‘ion-ion structure function.’’ When the positions of the ions are correlated (in the $T \rightarrow 0$ limit, they arrange themselves in a lattice), the ion-ion structure function reduces $\sigma_{\nu+A}$ substantially below $\sigma_{\nu+A}^0$ at low neutrino energies (*i.e.*, neutrino energies for which $\lambda_{\nu} > a$, where a is the interion spacing),

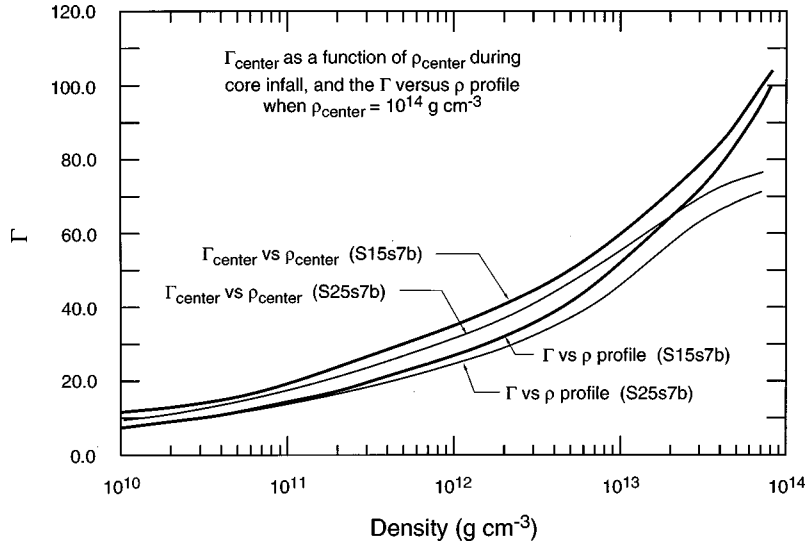


FIG. 1. The quantity Γ , defined in the text, at the core center for models S15s7b and S25s7b, as a function of the core-center density during infall; the Γ core profile when the core center reaches $10^{14} \text{ g cm}^{-3}$.

again because of destructive interference of the constituent amplitudes—the constituent amplitudes in this case being the scattering amplitudes from each ion.

The ion-ion structure function in the static approximation is a function of $\vec{q} = \vec{p}'_{\nu} - \vec{p}_{\nu}$, where \vec{p}'_{ν} and \vec{p}_{ν} are the final and initial neutrino momenta, respectively. We will denote the ion-ion structure function multiplying the differential cross section $d\sigma_{\nu+A}^0/d\Omega$ (or $d\sigma_{\nu+A}^1/d\Omega$) by $\mathcal{S}_{\text{ion}}(\vec{q})$. Extracting the angular variables from $\mathcal{S}_{\text{ion}}(\vec{q})$ and performing the angular integrations leaves a corresponding ion-ion correction multiplying $\sigma_{\nu+A}^0$ (or $\sigma_{\nu+A}^1$) that depends on the neutrino energy ϵ , which we will denote by $\langle \mathcal{S}_{\text{ion}}(\epsilon) \rangle$. The effect of the ion-ion correction $\langle \mathcal{S}_{\text{ion}}(\epsilon) \rangle$ on the deleptonization and hydrodynamics of the core during infall is the subject of this paper.

The dimensionless parameter Γ , which characterizes the strength of the ion-ion correlation, is the ratio of the unshielded electrostatic potential energy between two neighboring ions to the thermal energy, i.e.,

$$\Gamma = \frac{(Ze)^2}{a} \frac{1}{kT}, \quad (1)$$

where a is the mean interion distance given by

$$a = \left(\frac{4\pi}{3} n_{\text{ion}} \right)^{-1/3}, \quad (2)$$

and n_{ion} is the number density of ions, all assumed to have the same charge Z . A glance at Fig. 1 shows that the typical value of Γ for a massive stellar core during infall is between 20 and 40, suggesting that the ions are highly correlated and that the ion-ion structure function correction may be important. After core bounce and initial shock propagation, the situation changes. The bulk of the inner unshocked core is at densities exceeding ρ_{tr} , the nuclear matter transition density, and is composed of nuclear matter with $\Gamma \sim 0.1$. (The ions in this case are the individual protons.) The outer shocked core is composed of hot nucleons with $\Gamma \sim 0.01$. At most a very thin cold layer of material remains at the outer edge of the

inner core, with $\rho < \rho_{\text{tr}}$; this layer is initially composed of heavy nuclei, but is soon compressed by core contraction, and undergoes the transition to nuclear matter. Hence, NAS, and the ion-ion structure function correction, play an essential role in the evolution of the core only during infall.

Shortly after Freedman [18] pointed out the coherent aspect of NAS and its potential importance to the supernova problem, Itoh [21] cautioned that ion-ion correlations should be strong in the supernova core and that the ion-ion structure function will be an important correction to $\sigma_{\nu+A}^1$. He suggested that the Debye-Hückel approximation to the Monte Carlo results of Hansen [22] be used for $\mathcal{S}_{\text{ion}}(\vec{q})$, which is valid for low neutrino energies (specifically, for $qa/\hbar < 1.5$, where q is the magnitude of the neutrino momentum transfer). The angular integrations are easily performed to obtain $\langle \mathcal{S}_{\text{ion}}(\epsilon) \rangle$. Unfortunately, the restriction $qa/\hbar < 1.5$ is not satisfied during core collapse. More recently, Ichimaru, Iyetomi, and Tanaka [23] have provided tabulations of $\mathcal{S}_{\text{ion}}(\vec{q})$ that can be inserted in angular integrations to obtain $\langle \mathcal{S}_{\text{ion}}(\epsilon) \rangle$.

The effect on the evolution of the core during infall of including $\langle \mathcal{S}_{\text{ion}}(\epsilon) \rangle$ in $\sigma_{\nu+A}^1$ was first discussed briefly by Bowers and Wilson [12]. They found that including $\langle \mathcal{S}_{\text{ion}}(\epsilon) \rangle$ greatly increases the core deleptonization. However, their equation of state at that time did not give the correct nuclear abundance distribution [24]; consequently, the accuracy of this result is not clear. The effect of including $\langle \mathcal{S}_{\text{ion}}(\epsilon) \rangle$ was again briefly discussed by Bruenn [2], who used an expression constructed from Ichimaru *et al.*'s data. Figure 4 in Bruenn [2] presents a comparison of the results of core infall calculations with and without the inclusion of $\langle \mathcal{S}_{\text{ion}}(\epsilon) \rangle$, and indicates that the inclusion of $\langle \mathcal{S}_{\text{ion}}(\epsilon) \rangle$ leads to a modest increase in the deleptonization of the core [$\Delta Y_I = -0.02$, where ΔY_I is the difference between the trapped Y_I with and without the inclusion of $\langle \mathcal{S}_{\text{ion}}(\epsilon) \rangle$]. Recently Horowitz [25] introduced a fitting formula for $\langle \mathcal{S}_{\text{ion}}(\epsilon) \rangle$ based on his Monte Carlo calculations. Apparently unaware of the comparison given in Bruenn [2], he argued that the substantial reduction in $\sigma_{\nu+A}^1$ for low-energy neutri-

nos effected by $\langle \mathcal{S}_{\text{ion}}(\epsilon) \rangle$ would lead to a catastrophic deleptonization of the core during infall because higher-energy ν_e 's would downscatter by NES into a low-energy, ν_e -transparent ‘‘window’’ by ν_e -electron scattering, and then freely escape.

Because the effect on core infall of incorporating the factor $\langle \mathcal{S}_{\text{ion}}(\epsilon) \rangle$ in $\sigma_{\nu+A}^1$ has been discussed only briefly in the literature (viz., Bowers and Wilson [12], Bruenn [2]), the purpose of this paper is to address this issue in detail. Both for the sake of comparison and to better understand the role of coherent scattering and of all semileptonic neutral-current scattering processes in core collapse, we present the results that obtain if NAS is turned off completely, and the results that obtain if all semileptonic neutral-current scattering processes are turned off. In Sec. II we present comparisons of core infall results with and without the inclusion of $\langle \mathcal{S}_{\text{ion}}(\epsilon) \rangle$ in $\sigma_{\nu+A}^1$, as computed by Horowitz [25], and with other modifications to the neutrino scattering rates. In Sec. III we present a simple analytic model that reproduces the numerical results of Sec. III, and illustrates why the inclusion of $\langle \mathcal{S}_{\text{ion}}(\epsilon) \rangle$ in $\sigma_{\nu+A}^1$ does not result in catastrophic core deleptonization. Our conclusions are given in Sec. IV. In the Appendix, we present a derivation of the NAS rate used in our supernova code, which elucidates the origin of both the nuclear form factor and the ion-ion structure function $\langle \mathcal{S}_{\text{ion}}(\epsilon) \rangle$.

II. NUMERICAL SIMULATIONS

To determine the effect on the infalling core's deleptonization of incorporating the ion-ion structure function $\langle \mathcal{S}_{\text{ion}}(\epsilon) \rangle$ in $\sigma_{\nu+A}^1$, we have performed a number of numerical simulations with and without $\langle \mathcal{S}_{\text{ion}}(\epsilon) \rangle$, and with other modifications to the neutrino opacities. The latter were included to further elucidate the role of important neutrino opacities in core deleptonization. The simulations were performed with the supernova code described in Bruenn [9] and Bruenn and Haxton [26]. The Lattimer-Swesty equation of state [27] was used when the following two conditions were satisfied locally: (1) $n_B > 10^{-8} \text{ fm}^{-3}$ ($\rho > 1.67 \times 10^7 \text{ g cm}^{-3}$), where n_B is the number density of nucleons (free and bound) per cubic Fermi, and (2) $T > 4 \times 10^9 \text{ K}$, i.e., when the temperature is high enough for matter to be in nuclear statistical equilibrium (Thielemann, Nomoto, and Hashimoto [28]). The Baron-Copperstein-Kahana (BCK) equation of state (Cooperstein [29], Baron, Cooperstein, and Kahana [30,31]) was used when the second condition was satisfied, but not the first. If the second condition was not satisfied, the nuclei were treated as ideal gas particles (with excited states), and a nine species nuclear reaction network was used to follow the nuclear transmutations. Three-flavor multigroup flux-limited diffusion was used for the neutrino transport, with 20 energy zones spanning in geometric progression the neutrino energy range from 4 to 400 MeV. The calculations were initiated from the $15M_\odot$ precollapse model ‘‘S15s7b,’’ representative of a small-core model, and the $25M_\odot$ precollapse model ‘‘S25s7b,’’ representative of a large-core model, both provided by Woosley [32]. Some of their characteristics are listed in Table II.

As listed in Table III, five simulations were performed for each precollapse model. To describe these simulations, we

TABLE II. Precollapse models. ρ_{center} is the central density. s_{center} is the central dimensionless entropy per nucleon. $Y_{e \text{ center}}$ is the central electron fraction. M_{Fe} is the mass of the ‘‘iron’’ core (i.e., Y_e appreciably less than 0.5).

Model	$\rho_{\text{center}} \text{ (g cm}^{-3}\text{)}$	s_{center}	$Y_{e \text{ center}}$	$M_{\text{Fe}} \text{ (}M_\odot\text{)}$
S15s7b	9.05×10^9	0.779	0.4224	1.287
S25s7b	3.13×10^9	0.993	0.4300	1.785

begin with a list in Table IV of the standard neutrino interactions included in our supernova code. Simulations A incorporate all of these neutrino interactions and can be regarded as ‘‘standard’’ simulations *without* the ion screening correction factor $\langle \mathcal{S}_{\text{ion}}(\epsilon) \rangle$ multiplying $\sigma_{\nu+A}^1$. Simulations B can be regarded as ‘‘standard’’ simulations *with* the ion screening factor included; therefore a comparison of simulations A and B for a given precollapse model will show the effects on core infall of including the ion screening correction $\langle \mathcal{S}_{\text{ion}}(\epsilon) \rangle$. In simulations C, we have included the inelastic ν -A scattering cross sections computed by Haxton and described in Bruenn and Haxton [26]. If the effect of $\langle \mathcal{S}_{\text{ion}}(\epsilon) \rangle$ is to create a low-energy hole in the neutrino distribution, inelastic ν -A scattering will help to scatter ν_e 's into this hole during infall, with potentially important consequences for core deleptonization. The effect of $\langle \mathcal{S}_{\text{ion}}(\epsilon) \rangle$ is to reduce $\sigma_{\nu+A}^1$ at low neutrino energies, and simulations D show the consequences of setting $\sigma_{\nu+A}^1$ to zero altogether. Finally, all semileptonic neutral-current neutrino interactions are set to zero in simulations E, almost taking us back to Colgate and White [33] before neutral-current effects were incorporated in supernova simulations. (Neutral-current effects give only a slight modification to the pure lepton interactions, such as ν - e^- scattering, which is why in simulations E we are not taken back completely to Colgate and White [33].)

The effect of including $\langle \mathcal{S}_{\text{ion}}(\epsilon) \rangle$ in $\sigma_{\nu+A}^1$ is to dramatically reduce $\sigma_{\nu+A}^1$ at low neutrino energies. This is shown in Fig. 2, where, for selected central densities of simulations B, $\langle \mathcal{S}_{\text{ion}}(\epsilon) \rangle$ at the core center is given as a function of neutrino energy. $\langle \mathcal{S}_{\text{ion}}(\epsilon) \rangle$ causes a reduction in $\sigma_{\nu+A}^1$ at the lowest neutrino energy (4 MeV) of almost an order of magnitude for $\rho = 10^{11} \text{ g cm}^{-3}$ to well over two orders of magnitude for densities between 10^{13} and $10^{14} \text{ g cm}^{-3}$.

The implications of this reduction for neutrino transport during core infall can be ascertained by considering its effect on the transport optical depth, defined by

$$\tau_{\text{transport}}(\epsilon) = \int_0^{R_{\text{surface}}} \frac{dr}{\lambda_{\text{transport}}(r, \epsilon)}. \quad (3)$$

Here $\lambda_{\text{transport}}(r, \epsilon)$ relates in the diffusion approximation the first angular moment of the neutrino distribution function [which is proportional to the neutrino flux $\mathcal{F}(\epsilon)$] to the gradient of the zeroth angular moment [which is proportional to the neutrino energy density $u(\epsilon)$] by the diffusionlike equation

$$\mathcal{F}(r, \epsilon) = \frac{c \lambda_{\text{transport}}(r, \epsilon)}{3} \frac{\partial u(r, \epsilon)}{\partial r}. \quad (4)$$

TABLE III. Simulations.

Simulation	Neutrino interactions modified
A: No ion screening	$\sigma_{\nu+A}$ as given by Eq. (A49) i.e., without the inclusion of $\langle S_{\text{ion}}(\epsilon) \rangle$
B: Ion screening (Horowitz)	$\sigma_{\nu+A}$ as given by Eq. (A51) with $\langle S_{\text{ion}}(\epsilon) \rangle$ given by Horowitz [25]
C: Ion screening (Horowitz) and ν -nucleus inelastic scattering	Simulation B with the additional inclusion of ν -nucleus inelastic scattering as described in Bruenn and Haxton [26]
D: No ν -nucleus scattering	$\sigma_{\nu+A}$ is set to zero
E: No semileptonic neutral current scattering	Scattering cross sections of ν 's with nucleons, free or bound (i.e., interactions c–f in Table IV), are set to zero

In our supernova code, the contribution of NAS to $1/\lambda_{\text{transport}}$ is given by the coefficient of $\psi^{(1)}$ in Eq. (A45).

The effect of $\langle S_{\text{ion}}(\epsilon) \rangle$ on the transport optical depths at selected densities is shown for model S25s7b in Figs. 3(a)–3(d) by comparing the results of simulations A and B. Also shown in these figures are the transport optical depths for simulations D and E. When $\langle S_{\text{ion}}(\epsilon) \rangle$ is included, the total transport optical depth from the core center to the surface remains small until the central density exceeds $10^{12} \text{ g cm}^{-3}$, providing a low-energy window for neutrinos to escape. Note that at all central densities the reduction in $\tau_{\text{transport}}$ when $\langle S_{\text{ion}}(\epsilon) \rangle$ is included is less than it would be if $\tau_{\text{transport}}$ were simply multiplied by $\langle S_{\text{ion}}(\epsilon) \rangle$, i.e.,

$$\frac{\tau_{\text{transport}}(\epsilon)[\text{simulation B}]}{\tau_{\text{transport}}(\epsilon)[\text{simulation A}]} > \langle S_{\text{ion}}(\epsilon) \rangle. \quad (5)$$

There are two reasons for this: (1) $\tau_{\text{transport}}$ is an integral quantity, receiving contributions (in diminishing amounts) as we integrate from the core center to the surface. $\langle S_{\text{ion}}(\epsilon) \rangle$ is an increasing function of decreasing density (e.g., see Fig. 2); the value of $\langle S_{\text{ion}}(\epsilon) \rangle$ at the core center is therefore smaller than its average value along the radial path from the core center to the surface. For central densities between 10^{11} and $10^{12} \text{ g cm}^{-3}$, this is the principal reason for inequality (5). Turning NAS off altogether (simulation D) results in a substantial additional reduction in $\tau_{\text{transport}}$ for the above range of central densities, because $\sigma_{\nu+A}$ is zero throughout the core, rather than just very small near the core center. (2) At high densities (10^{13} – $10^{14} \text{ g cm}^{-3}$), the opacity due to

TABLE IV. Neutrino interactions. ν refers to a neutrino or antineutrino of any flavor.

a: $\nu_e + n \rightleftharpoons e^- + p$	electron neutrino–free neutron absorption
b: $\bar{\nu}_e + p \rightleftharpoons e^+ + n$	electron antineutrino–free proton absorption
c: $\nu + n \rightleftharpoons \nu + n$	neutrino–free neutron scattering
d: $\nu + p \rightleftharpoons \nu + p$	neutrino–free proton scattering
e: $\nu + \alpha \rightleftharpoons \nu + \alpha$	neutrino– α particle scattering
f: $\nu + A \rightleftharpoons \nu + A$	neutrino–heavy nucleus scattering (NAS)
g: $\nu + e^- \rightleftharpoons \nu + e^-$	neutrino–electron scattering (NES)
h: $\nu + e^+ \rightleftharpoons \nu + e^+$	neutrino–positron scattering
i: $\nu + \bar{\nu} \rightleftharpoons e^- + e^+$	neutrino–antineutrino pair annihilation

NES at the lowest neutrino energies is comparable to that of NAS. This is because the contribution of NES to $1/\lambda_{\text{transport}}$ goes as

$$\frac{1}{\lambda_{\text{transport}}|_{\nu-e^-}} = \frac{2\pi}{c(2\pi\hbar c)^3} \int_0^\infty d\epsilon' \{ \Phi_{0,\text{NES}}^{\text{in}}(\epsilon, \epsilon') \psi^0(\epsilon') + \Phi_{0,\text{NES}}^{\text{out}}(\epsilon, \epsilon') [1 - \psi^0(\epsilon')] \}, \quad (6)$$

where $\psi^0(\epsilon)$ is the zeroth angular moment of the neutrino distribution functions, and $\Phi_{0,\text{NES}}^{\text{in}}(\epsilon, \epsilon')$ and $\Phi_{0,\text{NES}}^{\text{out}}(\epsilon, \epsilon')$ are the zeroth angular moments of the ‘‘in’’ and ‘‘out’’ scattering kernels, respectively [9]. The very high rate of ν_e ‘‘in’’ scattering at the low end of the ν_e energy spectrum results in the large contribution of NES to $\tau_{\text{transport}}$. [This somewhat counterintuitive result can be understood by referring to Eq. (4). A large value for $\Phi_{0,\text{NES}}^{\text{in}}$ tends to produce both a larger magnitude and a greater isotropization of the neutrino distribution. This increases the neutrino energy density $u(r, \epsilon)$ more than the flux $\mathcal{F}(r, \epsilon)$, and therefore tends to decrease $\lambda_{\text{transport}}$, as defined by Eq. (4), thereby increasing $\tau_{\text{transport}}$.] In fact, at high densities and low ν_e energies, NAS no longer dominates $\tau_{\text{transport}}$, and the effect on $\tau_{\text{transport}}$ of

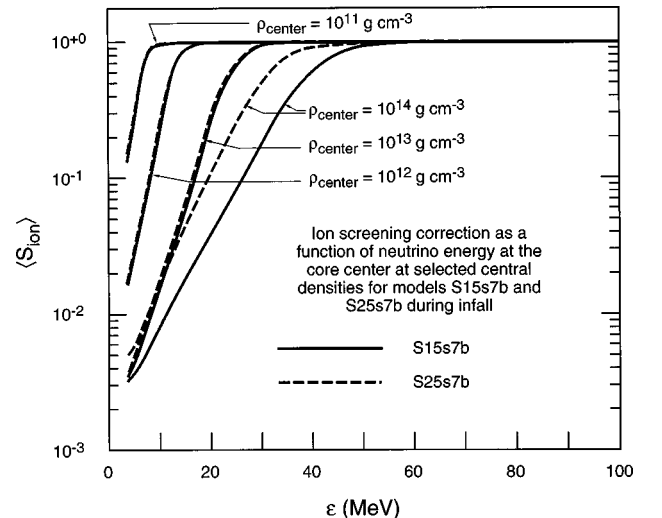


FIG. 2. The angle-averaged ion screening correction $\langle S_{\text{ion}}(\epsilon) \rangle$ at the core center for selected central densities, as a function of neutrino energy, for models S15s7b and S25s7b.

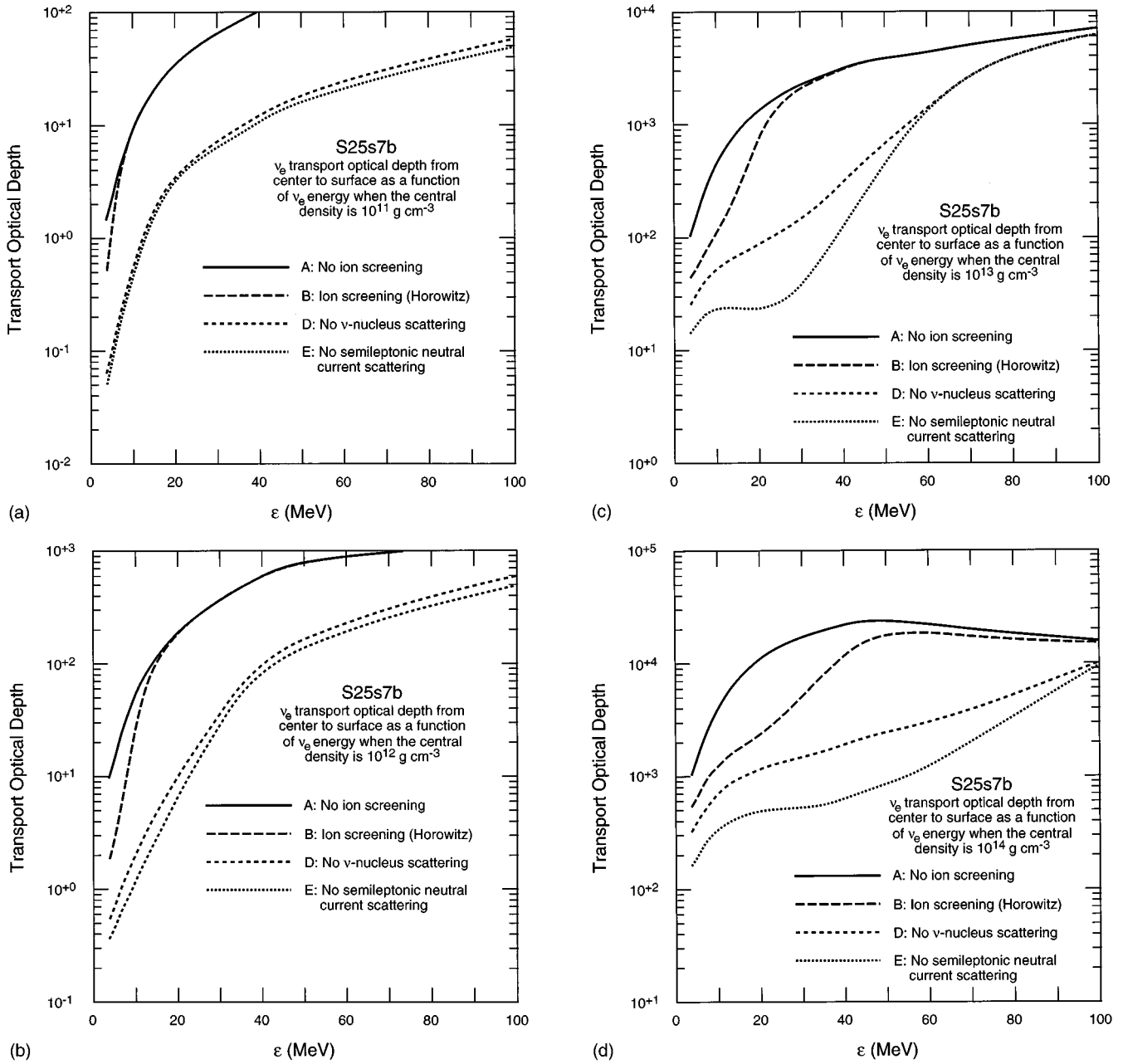


FIG. 3. The ν_e transport optical depths along a radial path from the core center to the surface for model S25s7b, as computed in simulations A, B, D, and E when the central density is (a) $10^{11} \text{ g cm}^{-3}$, (b) $10^{12} \text{ g cm}^{-3}$, (c) $10^{13} \text{ g cm}^{-3}$, and (d) $10^{14} \text{ g cm}^{-3}$.

the reduction in $\sigma_{\nu+A}^1$ due to $\langle S_{\text{ion}}(\epsilon) \rangle$ is correspondingly diminished. Figures 3(a)–3(d) also show that a further reduction in $\tau_{\text{transport}}$ at low ν_e energies occurs when NAS is turned off, and again when all semileptonic neutral-current scattering is turned off. These additional reductions in $\tau_{\text{transport}}$ arise not so much because of corresponding reductions in the low- ν_e -energy coherent scattering and semileptonic neutral-current scattering cross sections, but because of the importance of NES at low ν_e energies (and high densities). Turning off NAS and then all semileptonic neutral-current scattering reduces the opacities primarily at the intermediate and high ν_e energies (they are already small at low ν_e energies) and causes the core to undergo substantially more de-leptonization during infall. With fewer electrons remaining to contribute to NES at low ν_e energies, $\tau_{\text{transport}}$ is correspondingly reduced there.

For various modifications to the neutrino opacities, Figs. 4(a), 4(b), 5(a), and 5(b) show the consequences for core de-leptonization during the core collapse of models S15s7b and S25s7b. Our main conclusion follows from a comparison of simulations A and B, from which it is evident that the effect of including $\langle S_{\text{ion}}(\epsilon) \rangle$ is a rather mild reduction of the trapped lepton fraction Y_l . This reduction in Y_l is about 0.015 for both models. Including the ν -A inelastic scattering computed by Haxton [26] reduces the trapped Y_l by an additional negligible amount. Substantial reductions in Y_l occur if NAS is turned off completely, and particularly if all semileptonic neutral-current scattering is turned off. This last result is the modern equivalent of the original Colgate and White [33] calculation. It shows that modern neutrino transport, with late 1960s neutrino physics, leads to a trapped lepton fraction of 0.18 rather than a value close to zero as

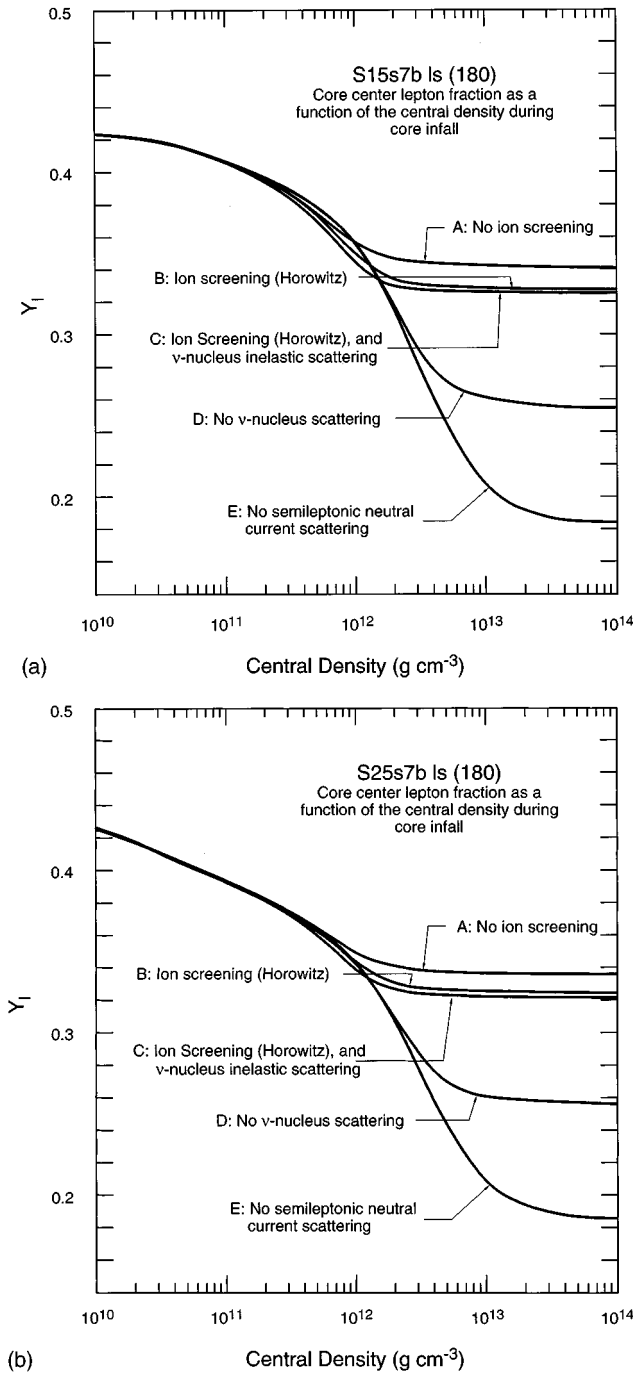


FIG. 4. The core-center lepton fraction as a function of central density during infall, in each of the five simulations, for (a) model S15s7b and (b) model S25s7b.

suggested by Colgate and White ([33], p. 651).

It might be suggested that the lack of extensive additional depletion when ion screening corrections are included results because the low-energy neutrino states, which are the states most affected by ion screening, are simply not populated. Several neutrino processes are important in filling the low-energy ν_e window during core collapse. Figures 6(a) and 6(b) show “net” production of ν_e 's (i.e., gains minus losses) for the most important ν_e production processes, at densities of 10^{11} and $10^{12} \text{ g cm}^{-3}$, respectively. With the exception at $10^{11} \text{ g cm}^{-3}$ at the lowest neutrino energies, NES

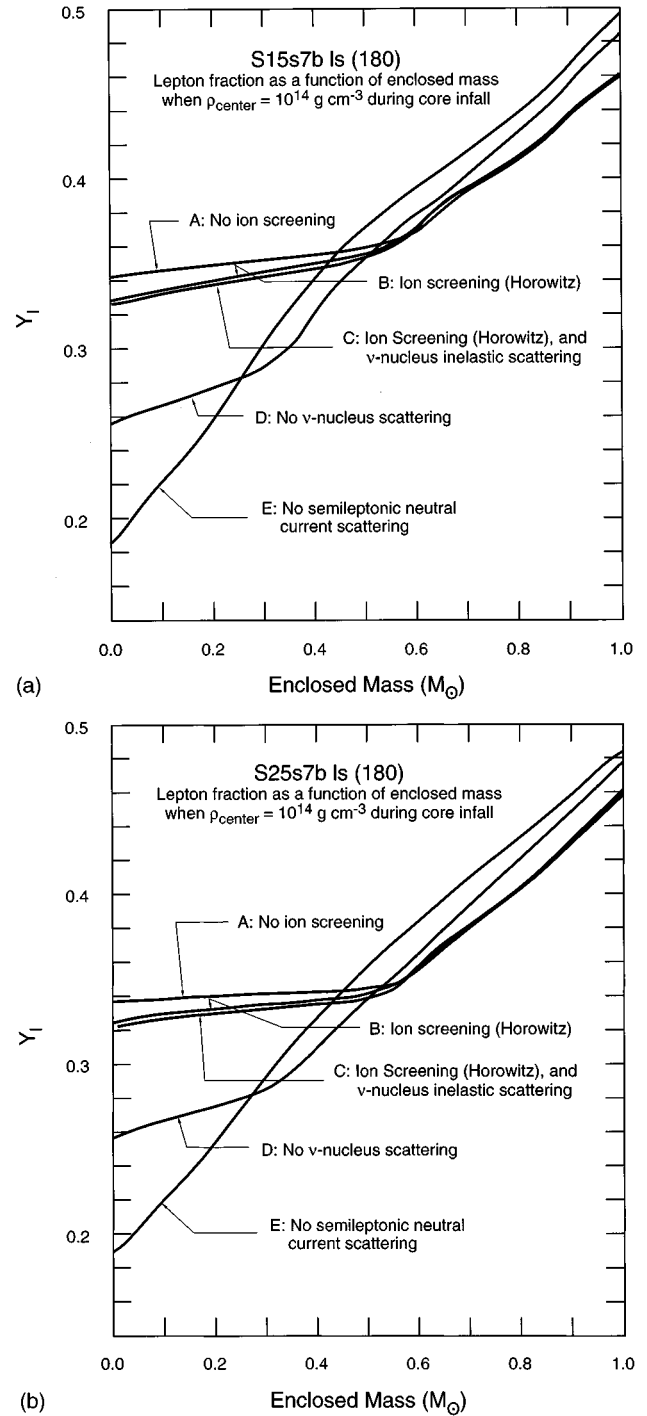


FIG. 5. The lepton fraction profiles in each of the five simulations when the central densities reach $10^{14} \text{ g cm}^{-3}$ for (a) model S15s7b and (b) model S25s7b.

is the dominant process, followed by ν -A inelastic scattering. The net production of low-energy ν_e 's by NES is sufficiently rapid that the low-energy window is completely filled shortly after the central density reaches $10^{12} \text{ g cm}^{-3}$. This is shown for simulations A, B, and E by Figs. 7(a)–7(c), respectively, which show the angle-averaged neutrino occupation number $\psi^{(0)}$ at selected densities during infall. At $10^{12} \text{ g cm}^{-3}$, $\psi^{(0)}$ is somewhat reduced at low energies when $\langle \mathcal{S}_{\text{ion}}(\epsilon) \rangle$ is included [simulation B, Fig. 7(b)] relative to its values when $\langle \mathcal{S}_{\text{ion}}(\epsilon) \rangle$ is omitted [simulation A, Fig. 7(a)], whereas at the

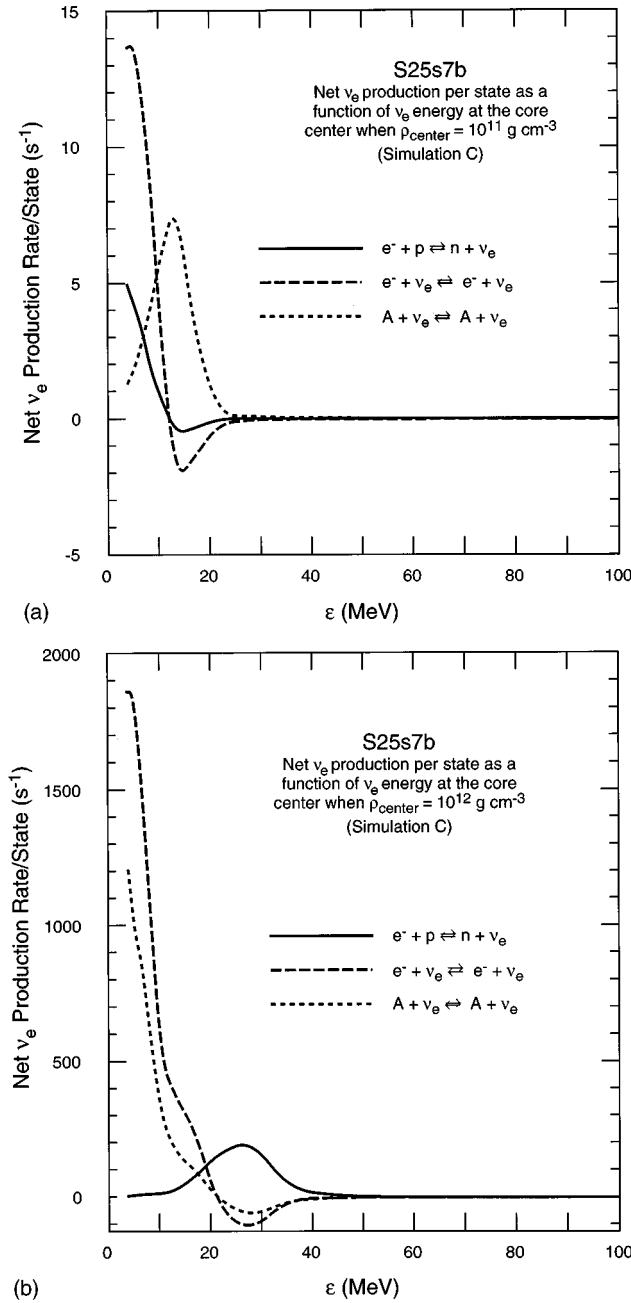


FIG. 6. The net ν_e production per state (i.e., gains minus losses) at the core center, as a function of ν_e energy, resulting from ν_e absorption and emission on free nucleons, elastic scattering on electrons, and inelastic scattering on nuclei. These were computed in simulation C for model S25s7b, when the central density reached (a) $10^{11} \text{ g cm}^{-3}$, and (b) $10^{12} \text{ g cm}^{-3}$.

same central density, $\psi^{(0)}$ is substantially reduced when all semileptonic neutral-current scattering is turned off [simulation E, Fig. 7(c)]. However, by $10^{13} \text{ g cm}^{-3}$, the low-energy ν_e states are completely filled in all simulations. Therefore there must be another reason for the lack of additional depletion when ion screening corrections are included. The fundamental reason, which will be elucidated in the next section by our analytic model, is this: Even if all the neutrino states below a low-energy threshold were populated and these neutrinos were allowed to freely escape from the core, there simply would not be enough states in this low-energy

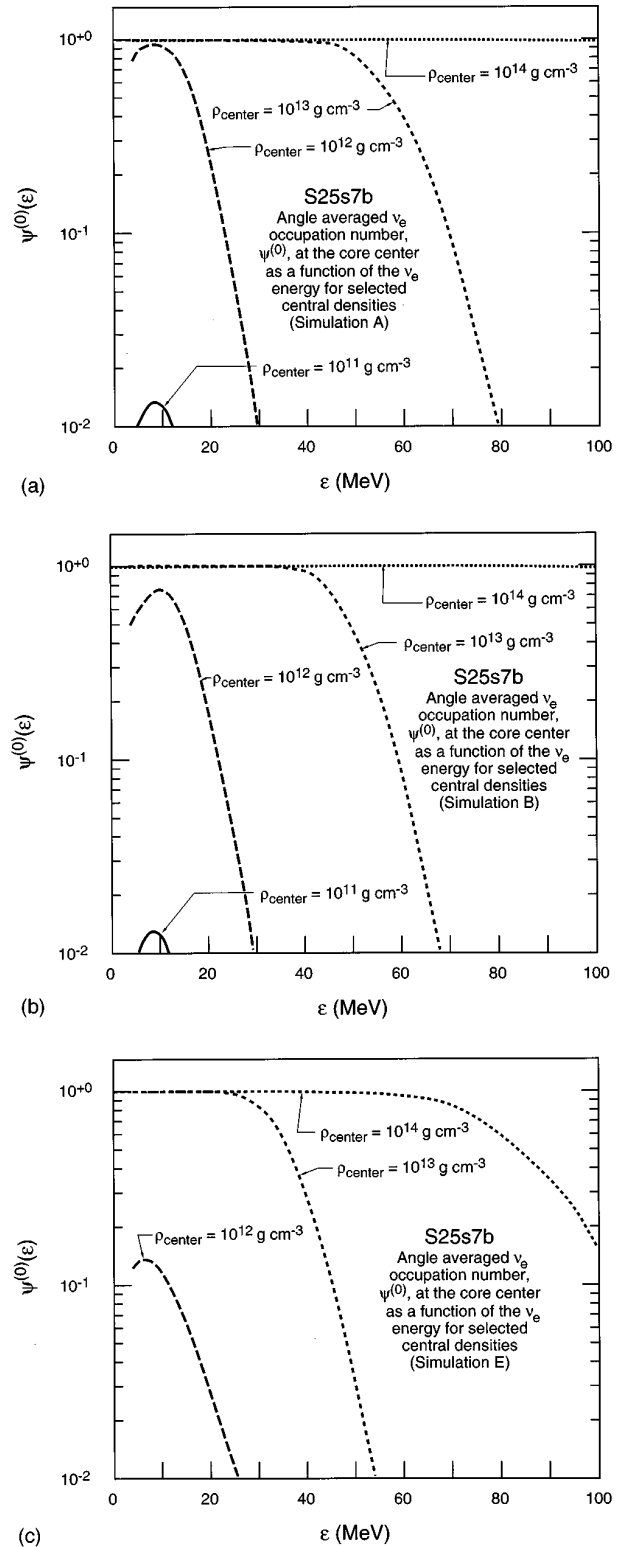


FIG. 7. The angle-averaged ν_e occupation number at the core center at select central densities, as a function of ν_e energy, for model S25s7b in (a) simulation A, (b) simulation B, and (c) simulation E.

window to result in a significant reduction in the core lepton fraction.

Figures 8(a) and 8(b) show the entropy of the central zones of models S15s7b and S25s7b, respectively, as a function of central density during collapse. The entropy produc-

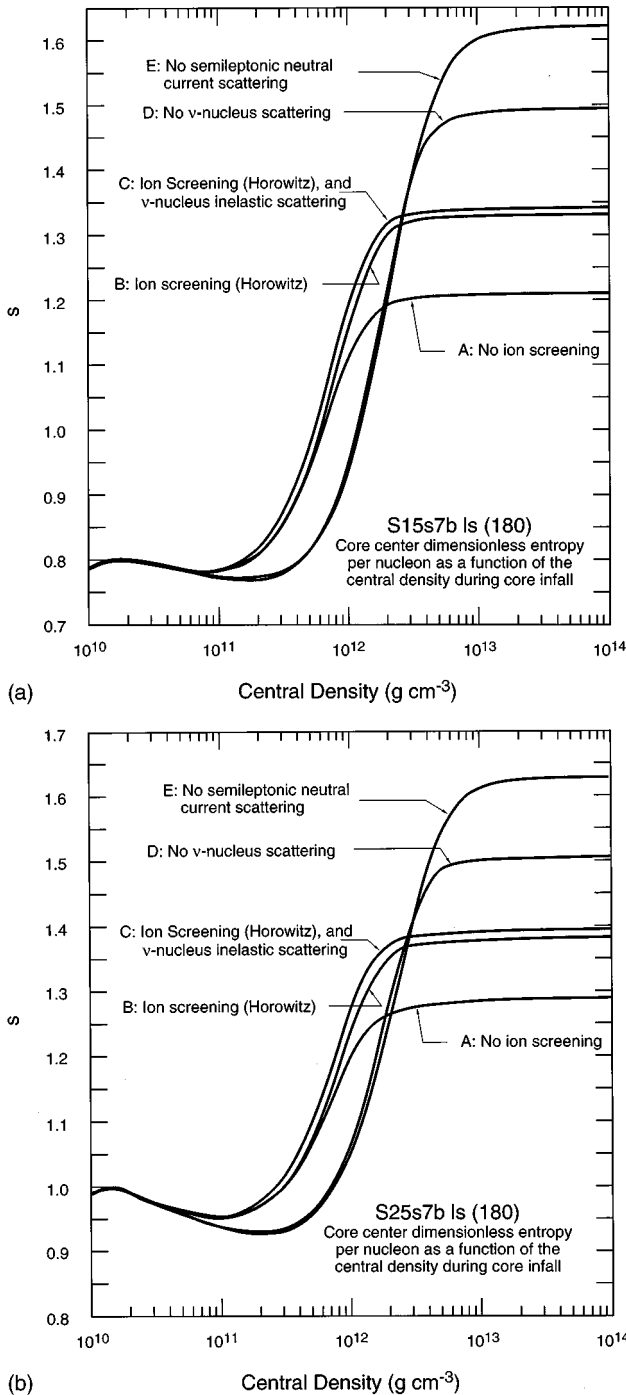


FIG. 8. The core-center dimensionless entropy as a function of central density during infall, in each of the five simulations, for (a) model S15s7b and (b) model S25s7b.

tion during core infall has been discussed by a number of people (Arnett [34], Epstein and Pethick [35], Van Riper and Lattimer [36], Bludman, Lichtenstadt, and Hayden [37], Bruenn [9]). No shocks are present, and the change in the matter entropy is due almost entirely to weak interactions. These, unlike the strong and electromagnetic interactions, are not equilibrated during infall. The entropy production depends on the number of ν_e 's produced per baryon, and increases as the energy of the ν_e 's emitted from the core decreases [see, e.g., Bruenn [9], Eqs. (3.13)–(3.15)]. The sensitive dependence of the free-proton abundance on the

entropy means that the core entropy change during infall has an important effect on core deleptonization if this entropy change occurs before neutrino trapping. Entropy generation and deleptonization are linked in a positive feedback loop: Entropy generation increases the free-proton fraction, which increases the electron capture rate, which increases the core deleptonization, which, completing the loop, produces more entropy. This positive feedback loop is quenched once the neutrinos become trapped. The transport optical depths shown in Figs. 3(a)–3(d) demonstrate that, before core bounce, these optical depths become large for all neutrino energies and for all simulations. Therefore neutrinos of all energies become trapped before core bounce, even those in simulations E in which all semileptonic neutral-current scattering is turned off. The trapping and equilibration of neutrinos with matter at high densities is evident for all simulations in Figs. 8(a) and 8(b), as the entropy versus density curves level off at high densities.

Comparisons of the entropy trajectories given by simulations B (or C) with those given by A show that the inclusion of $\langle S_{\text{ion}}(\epsilon) \rangle$ leads to considerably increased entropy production during infall, despite the rather mild increase in core deleptonization. This is because the inclusion of $\langle S_{\text{ion}}(\epsilon) \rangle$ increases the tendency for low-energy ν_e 's to escape. The result is a lowering of the mean energy of the emitted ν_e 's from 9.47 to 9.11 MeV for model S15s7b, when $\rho_{\text{center}} = 10^{12} \text{ g cm}^{-3}$, and at a similar epoch, from 9.33 to 9.28 MeV for model S25s7b. On the other hand, for simulations D and E, the mean energy of the emitted ν_e 's for model S15s7b increases to 11.27 and 11.34 MeV, respectively, and for model S25s7b to 10.72 and 10.81 MeV, respectively. The increased entropy production exhibited by these latter simulations is due entirely to increased core deleptonization.

The consequence for core hydrodynamics of including $\langle S_{\text{ion}}(\epsilon) \rangle$ is shown in Table V, where the quantity M_{shock} is given for each simulation. Here M_{shock} is the mass enclosed by the bounce shock when it forms. The location at which it first forms is defined as the radius at which the dimensionless matter entropy per baryon first achieves a value of 3. The larger the value of M_{shock} , the greater the strength of the shock, and the less ironlike material it must encounter and dissociate before it propagates out through the rest of the core. The value of M_{shock} is therefore an indicator of how far out the shock will propagate before stalling. It is seen from Table V that including $\langle S_{\text{ion}}(\epsilon) \rangle$ reduces M_{shock} by 2.3% and 5.7% for models S15s7b and S25s7b, respectively. The inclusion of inelastic neutrino-nucleus scattering reduces M_{shock} further by $\sim 1\%$. Substantial reductions in M_{shock} occur only when neutrino-nucleus elastic scattering is turned off, and particularly when semileptonic neutral currents are turned off.

We summarize this section by noting that the inclusion of $\langle S_{\text{ion}}(\epsilon) \rangle$ in the neutrino-nucleus scattering opacity has a mild, rather than a dramatic, effect on core hydrodynamics. Why the core does not deleptonize more when $\langle S_{\text{ion}}(\epsilon) \rangle$ is included, with greater consequences for the subsequent core hydrodynamics, is not because ν_e 's are not rapidly down-scattered into the low-energy window created by $\langle S_{\text{ion}}(\epsilon) \rangle$; it is because the low-energy window affected by $\langle S_{\text{ion}}(\epsilon) \rangle$ is too narrow. We will demonstrate this in the next section by introducing a simple model.

TABLE V. Mass enclosed by shock.

Simulation	$M_{\text{shock, S15s7b}}$	$M_{\text{shock, S25s7b}}$
A: No ion screening	0.6008	0.6425
B: Ion screening (Horowitz)	0.5868	0.6061
C: Ion screening (Horowitz) and ν -nucleus inelastic scattering	0.5804	0.5988
D: No ν -nucleus scattering	0.4412	0.4480
E: No semileptonic neutral current scattering	0.3506	0.3565

III. ANALYTIC MODEL

To elucidate the effect ion screening corrections have on the deleptonization of a stellar core during infall, we develop a simple analytic model. We begin by deriving a general expression for the change in the mean core lepton fraction $\langle Y_l(t) \rangle$ within a fixed radius R at time t as a result of including ion screening corrections. $\langle Y_l(t) \rangle$ is given by

$$\langle Y_l(t) \rangle \equiv \frac{N_l(t)}{N_B(t)} = \frac{N_{l_i} + \int_0^t \dot{N}_l(t') dt'}{N_{B_i} + \int_0^t \dot{N}_B(t') dt'}, \quad (7)$$

where $N_l(t)$ and $N_B(t)$ are the lepton and baryon numbers inside R at time t ; N_{l_i} and N_{B_i} are the initial lepton and baryon numbers inside R , and $\dot{N}_l(t')$ and $\dot{N}_B(t')$ are the rates of inflow through R of leptons and baryons. We decompose $\dot{N}_l(t')$ to $\dot{N}_l^{(\text{in})}(t') - \dot{N}_l^{(\text{out})}(t') - \dot{N}_{l(\text{ion-ion})}^{(\text{out})}(t')$, where $\dot{N}_l^{(\text{in})}(t')$ is the rate at which leptons are advected inward through R with the matter, $\dot{N}_l^{(\text{out})}(t')$ is the rate at which neutrino transport without ion screening causes leptons (i.e., ν_e 's minus $\bar{\nu}_e$'s) to flow out of R , and $\dot{N}_{l(\text{ion-ion})}^{(\text{out})}(t')$ is the additional rate of lepton flow out of R when ion screening is included. To simplify the analysis, we assume that the hydrodynamics is the same with or without ion screening. (This is justified *a posteriori* by the small effect ion screening corrections will be shown to have on core deleptonization.) Use of the above decomposition in Eq. (7) gives

$$\langle Y_l(t) \rangle = \frac{N_{l_i} + \int_0^t [\dot{N}_l^{(\text{in})}(t') - \dot{N}_l^{(\text{out})}(t') - \dot{N}_{l(\text{ion-ion})}^{(\text{out})}(t')] dt'}{N_{B_i} + \int_0^t \dot{N}_B(t') dt'}. \quad (8)$$

From Eq. (8) it is clear that the additional deleptonization due to ion screening is given by

$$\langle \Delta Y_l(t) \rangle = \frac{- \int_0^t \dot{N}_{l(\text{ion-ion})}^{(\text{out})}(t') dt'}{N_{B_i} + \int_0^t \dot{N}_B(t') dt'}. \quad (9)$$

Equation (9) can be written in a form that is useful for approximation. We note first that, if time $t'=0$ corresponds to the initiation of core collapse and $t'=t$ to core bounce, and if R is chosen to be fixed (time independent) at the mean ν_e -sphere radius R_{ν_e} during core collapse, the mean density $\langle \rho \rangle$ inside R_{ν_e} increases from $\sim 10^{10} \text{ g cm}^{-3}$ at $t=0$ to $\sim 10^{14} \text{ g cm}^{-3}$ at time t . Because R_{ν_e} is fixed, N_B scales with $\langle \rho \rangle$; therefore $N_{B_i} \ll N_B(t) = N_{B_i} + \int_0^t \dot{N}_B(t') dt'$, and N_{B_i} is negligible in comparison with $\int_0^t \dot{N}_B(t') dt'$, and will be dropped. We next replace the ratio of the integrals in Eq. (9) by the ratio of the time-averaged values of the integrands. The result is

$$\langle \Delta Y_l(t) \rangle \approx \frac{- \int_0^t \dot{N}_{l(\text{ion-ion})}^{(\text{out})}(t') dt'}{\int_0^t \dot{N}_B(t') dt'} = \frac{- \langle \dot{N}_{l(\text{ion-ion})}^{(\text{out})} \rangle}{\langle \dot{N}_B \rangle}. \quad (10)$$

An approximation for $\langle \Delta Y_l(t) \rangle$ will now be obtained by deriving numerical estimates of $\langle \dot{N}_{l(\text{ion-ion})}^{(\text{out})} \rangle$ and $\langle \dot{N}_B \rangle$.

An estimate of $\langle \dot{N}_B \rangle$ can be obtained by considering the inflow of baryons through R_{ν_e} , i.e.,

$$\begin{aligned} \langle \dot{N}_B \rangle &= \frac{\rho(R_{\nu_e})}{m_B} v 4\pi R_{\nu_e}^2 = \frac{\rho(R_{\nu_e})}{m_B} \frac{1}{2} \sqrt{\frac{2Gm(R_{\nu_e})}{R_{\nu_e}}} 4\pi R_{\nu_e}^2 \\ &= 1.1 \times 10^{45} [m(R_{\nu_e})/M_\odot]^{1/2} R_{\nu_e,50}^{-1/2} 4\pi R_{\nu_e}^2, \end{aligned} \quad (11)$$

where we have used $\rho(R_{\nu_e}) = 5 \times 10^{11} \text{ g cm}^{-3}$, and half the free-fall velocity for v , in accordance with the results of similarity solutions for the infall of the outer core [7]. During core infall, the ν_e sphere forms at a mean radius $R_{\nu_e} \approx 50 \text{ km}$ and a mean density $\rho(R_{\nu_e}) \approx 5 \times 10^{11} \text{ g cm}^{-3}$. This radius and density appear to be insensitive to both the pre-collapse model and the time during infall [38].

To estimate $\langle \dot{N}_{l(\text{ion-ion})}^{(\text{out})} \rangle$, we note that ion screening's effect is to greatly reduce the ν_e -nucleus scattering cross section for low-energy ν_e 's. We therefore make the assumption that the consequence of including ion screening is to allow all the ν_e 's with $\epsilon_{\nu_e} < \epsilon_{\nu_e, \text{max}}$ to rapidly escape from the core. To estimate $\epsilon_{\nu_e, \text{max}}$, we note that the main ν_e opacity source during infall is NAS, which corresponds to the transport mean free path derived by Brown, Bethe, and Baym [39];

$$\lambda^t = \frac{15.2}{\epsilon_{\nu_e,10}^2 \rho_{12} A C^2 \langle \mathcal{S}_{\text{ion}}(\epsilon) \rangle} \text{ km}, \quad (12)$$

where $\epsilon_{\nu_e,10} = \epsilon_{\nu_e} / (10 \text{ MeV})$. The mean density below the ν_e sphere, ρ_{12} , is given by

$$\rho_{12} = 3.8 \frac{m(R_{\nu_e})/M_\odot}{R_{\nu_e,50}^3}, \quad (13)$$

where $\rho_{12} = \rho / (10^{12} \text{ g cm}^{-3})$, $R_{\nu_e,50} = R_{\nu_e} / (50 \text{ km})$, and $m(R_{\nu_e})$ is the time-dependent mass enclosed within R_{ν_e} . C^2 is the weak coupling strength, which for $A=120$ and Z

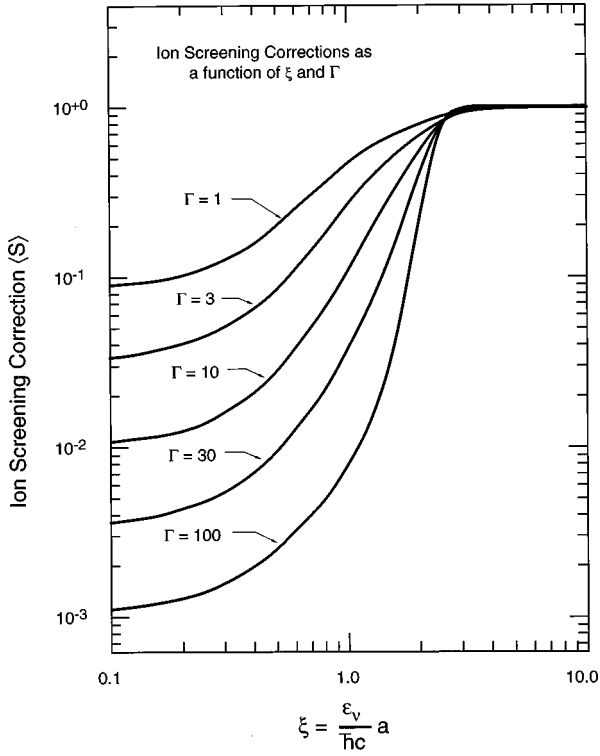


FIG. 9. The angle-averaged ion screening correction $\langle S_{\text{ion}}(\epsilon) \rangle$ as a function of ξ , the ratio of the ν_e Compton wavelength to the mean ion-ion separation, and Γ , the ratio of the ion-ion Coulomb potential energy to the ion thermal energy.

$=40$ is 0.0756 (A and Z of the typical heavy nucleus increase slowly towards the center with $A \sim 120$ and $Z \sim 40$ as representative means [27]). $\langle S_{\text{ion}}(\epsilon) \rangle$ is the angle-averaged ion screening correction to the ν_e -nucleus scattering cross section, and is approximated by Horowitz [25] using the following function of ξ and Γ :

$$\langle S_{\text{ion}}(\epsilon) \rangle = \frac{1}{1 + \exp\left(-\sum_{i=0}^6 \beta_i(\Gamma) \xi^i\right)}, \quad (14)$$

where ξ is the ratio of the mean ion-ion separation a to the ν_e Compton wavelength, i.e.,

$$\xi = a \frac{\epsilon_{\nu_e}}{\hbar c}, \quad (15)$$

where a is given by Eq. (2). Γ is the ratio of the ion-ion Coulomb potential to the thermal energy, and is given by Eq. (1), and the β_i are specified functions of Γ , obtained by least-squares fits of $\langle S_{\text{ion}}(\epsilon) \rangle$ to Monte Carlo data. A glance at Fig. 9 shows that $\langle S_{\text{ion}}(\epsilon) \rangle$ is a very sensitive function of ξ , with $\langle S_{\text{ion}}(\epsilon) \rangle \ll 1$ for $\xi \lesssim 1$, if $\Gamma \gtrsim 10$.

To determine $\epsilon_{\nu_e \text{ max}}$, we express $\epsilon_{\nu_e 10}$ in Eq. (12) in terms of ξ and the mean ρ and A below R_{ν_e} , and determine the value of ξ below which ν_e 's can freely escape from the core. (The escape criterion will be expressed in terms of λ^t .) Solving Eq. (15) for ϵ_{ν_e} , and using Eqs. (2) and (13), we obtain

$$\epsilon_{\nu_e 10} = 0.544 \left(\frac{\rho_{12}}{A_{120}} \right)^{1/3} \xi = 0.85 \frac{1}{R_{\nu_e 50}} \left(\frac{m(R_{\nu_e})/M_{\odot}}{A_{120}} \right)^{1/3} \xi, \quad (16)$$

where $A_{120} = A/120$. Using Eq. (16) in Eq. (12) gives

$$\lambda^t = \frac{0.607 R_{\nu_e 50}^5}{[m(R_{\nu_e})/M_{\odot}]^{5/3} A_{120}^2 \langle S_{\text{ion}}(\epsilon) \rangle} \text{ km}. \quad (17)$$

We now assert that neutrinos will rapidly escape from the core if

$$\lambda^t \gtrsim \zeta R_{\nu_e}, \quad (18)$$

where ζ is of order unity. Inequality (18) will be satisfied for $\xi < \xi_{\text{max}}$, where ξ_{max} is obtained by treating inequality (18) as an equality. The ion screening correction $\langle S_{\text{ion}}(\epsilon) \rangle$ depends on ξ and Γ , defined in Eqs. (15) and (1), respectively. We observe from Fig. 1 that the quantity Γ increases with increasing density during core infall, with a typical value being ~ 35 . Choosing $\Gamma = 35$, the solution of Eq. (18) for ξ_{max} , with $R_{\nu_e 50} = 1$, $m(R_{\nu_e})/M_{\odot} = 0.7$, $A_{120} = 1$, gives $\xi_{\text{max}} = 0.933$ and 1.486 for representative values of ζ of 1 and 1/10, respectively. From Eq. (16), values of 0.933 and 1.486 for ξ_{max} give $\epsilon_{\nu_e \text{ max}} = 7.0$ and 11.2 MeV, respectively.

If we assume that the effect of ion screening is to allow all ν_e 's with $\epsilon_{\nu_e} < \epsilon_{\nu_e \text{ max}}$ to freely escape, and assume further that ν_e downscattering on electrons is sufficiently rapid to completely populate these ν_e states below R_{ν_e} , the radiation of ν_e 's with $\epsilon_{\nu_e} < \epsilon_{\nu_e \text{ max}}$ will occur at the blackbody rate; i.e., their number flux will be equal to $(c/4)n_{\nu_e}$, with the number density of ν_e 's with $\epsilon_{\nu_e} < \epsilon_{\nu_e \text{ max}}$ given by the completely degenerate maximum, $n_{\nu_e} = (4\pi/3)[\epsilon_{\nu_e \text{ max}}^3/(hc)^3]$. This provides an upper bound for $\langle \dot{N}_{\text{ion-ion}}^{\text{(out)}} \rangle$, given by

$$\begin{aligned} \langle \dot{N}_{\text{ion-ion}}^{\text{(out)}} \rangle &= \frac{c}{4} n_{\nu_e} 4\pi R_{\nu_e}^2 = \frac{c}{4} \frac{4\pi}{3} \frac{\epsilon_{\nu_e \text{ max}}^3}{(hc)^3} 4\pi R_{\nu_e}^2 \\ &= 1.64 \times 10^{43} \left(\frac{\epsilon_{\nu_e \text{ max}}}{10 \text{ MeV}} \right)^3 4\pi R_{\nu_e}^2 \\ &= \begin{cases} 5.62 \times 10^{42} 4\pi R_{\nu_e}^2, & \zeta = 1 \\ 2.30 \times 10^{43} 4\pi R_{\nu_e}^2, & \zeta = \frac{1}{2} \end{cases}. \end{aligned} \quad (19)$$

Using Eqs. (19) and (11) in Eq. (10) and taking $R_{\nu_e 50} = 1$ and $m(R_{\nu_e})/M_{\odot} = 0.7$ gives

$$\langle \Delta Y_l(t) \rangle \approx \begin{cases} -0.0061, & \zeta = 1 \\ -0.025, & \zeta = \frac{1}{10} \end{cases}. \quad (20)$$

These two values bound our numerical results presented in the preceding section.

IV. SUMMARY AND CONCLUSIONS

On the basis of detailed numerical simulations of core infall presented in Sec. II and the simplified analytic model constructed in Sec. III, we draw the following conclusions.

(1) $\langle \mathcal{S}_{\text{ion}}(\epsilon) \rangle$ does in fact cause a drastic reduction in the NAS cross section, $\sigma_{\nu+A}(\epsilon)$, for low neutrino energies [i.e., for $\xi < 1$, cf., Eq. (15) and Figs. 2 and 9].

(2) The low-energy window created by the reduction in $\tau_{\text{transport}}(\epsilon)$ from ion screening is efficiently filled by ν_e 's downscattered by NES. By $\rho = 10^{12} \text{ g cm}^{-3}$, there is very little difference between the population of ν_e 's at the lowest energies, with or without the inclusion of $\langle \mathcal{S}_{\text{ion}}(\epsilon) \rangle$, and in both cases, the occupation of states is close to unity.

(3) The additional deleptonization resulting from the inclusion of $\langle \mathcal{S}_{\text{ion}}(\epsilon) \rangle$ is relatively small. We obtain a reduction in the trapped lepton fraction Y_l of about 0.015 for both the $15M_\odot$ and the $25M_\odot$ models.

(4) A simple analytic model demonstrates that the unexpectedly small additional deleptonization that results when $\langle \mathcal{S}_{\text{ion}}(\epsilon) \rangle$ is included is a consequence of the restricted phase space in the low-energy window; i.e., if $\tau_{\text{transport}}(\epsilon)$ is set to zero in the low-energy window, and NES is assumed sufficiently rapid to completely populate it with ν_e 's, the deleptonization that results is small and in accord with the deleptonization obtained in our detailed numerical simulations.

(5) The inclusion of $\langle \mathcal{S}_{\text{ion}}(\epsilon) \rangle$ reduces the mass initially enclosed by the bounce shock when it first forms, by 2.3% and 5.7% for the $15M_\odot$ and $25M_\odot$ models, respectively. This weakens the bounce shock and causes it to stagnate at smaller radii, but the effect is insignificant.

ACKNOWLEDGMENTS

S.W.B. was supported at Florida Atlantic University under NSF Grant No. AST-9618423 and NASA Grant No. NAG5-3903. A.M. was supported at the Oak Ridge National Laboratory, which is managed by Lockheed Martin Energy Research Corporation under U.S. DOE Contract No. DE-AC05-96OR22464. We would like to acknowledge stimulating conversations with Stirling Colgate. Some of the simulations presented here were performed on the Silicon Graphics Power Challenge at the Florida Supercomputer Center.

APPENDIX

We present here a derivation of the neutrino-nucleus elastic scattering cross section as it appears in our supernova code. The purpose is to include many of the details omitted from previous work, to make clear the approximations made in the final expression used in our supernova code, and to elucidate the origin and physical significance of both the nuclear and the ion static structure functions. Previous work begins with the recognition by Freedman [18] that the amplitudes for neutrino scattering on the nucleons in a nucleus should combine coherently. He calculated the cross section for neutrino scattering on spinless, $Z=A$ nuclei (for which only the isoscalar, vector current contributes), and suggested its importance to the neutrino transport attending stellar collapse. Tubbs and Schramm [10] extended the neutrino-nucleus elastic scattering cross section to spinless, $Z \neq A$ nuclei by adding the isovector, vector contribution to the

nuclear current. Both of the above cross sections included a nuclear form factor correction that reduces the cross section at high neutrino energies. Scattering kernels for neutrino transport codes based on the above formalism were computed by Yueh and Buchler [19] and Bruenn [9]. A clear discussion of coherent nuclear scattering and the nuclear form factor is given in Freedman, Schramm, and Tubbs [20].

We assume a medium occupying a volume V and consisting of N_{nuc} identical nuclei of charge Z and mass number A , immersed in a uniform electron sea. The transition rate for neutrino-nucleus scattering from a definite initial to a definite final state can be written in the low-energy (low-neutrino-energy) limit as an effective current-current interaction given by

$$w_{fi} = \frac{2\pi}{\hbar} \delta(E_{\text{nuc } f} - E_{\text{nuc } i} + E_{\nu f} - E_{\nu i}) |M|^2, \quad (\text{A1})$$

where

$$M = \frac{GL^\mu}{\sqrt{2}} \left\langle \Psi_f \left| \sum_{n=1}^{N_{\text{nuc}}} \sum_{j=1}^A \hat{J}_{\text{nuc } \mu}^{jn} \exp[(i/\hbar)\bar{q} \cdot \bar{r}_{jn}] \right| \Psi_i \right\rangle, \quad (\text{A2})$$

Ψ is the state of the medium, $\hat{J}_{\text{nuc } \mu}^{jn}$ is the nuclear neutral current operator for the j th nucleon of the n th nucleus, L^μ is the lepton matrix element, given by

$$L^\mu \equiv \langle \nu_f | \hat{L}^\mu | \nu_i \rangle = \frac{c^2}{V \sqrt{E_{\nu f} E_{\nu i}}} \bar{u}_{\nu_e}(\bar{p}_{\nu f}) \gamma^\mu (1 - \gamma_5) u_{\nu_e}(\bar{p}_{\nu i}), \quad (\text{A3})$$

and G is the effective weak coupling constant ($G = 8.99 \times 10^{-44} \text{ MeV cm}^3$ [40]). The spatial dependence, $\exp(i\bar{q} \cdot \bar{r}_{jn})$, of the neutrino plane wave states has been factored out of L^μ and appears explicitly in Eq. (A2). The quantity $\bar{q} = \bar{p}_{\nu i} - \bar{p}_{\nu f}$ is the momentum transfer from the neutrino to the medium, and is a c -number. The quantity \bar{r}_{jn} in Eq. (A2) and in what follows is an operator.

To construct $\hat{J}_{\text{nuc } \mu}^{jn}$, we use the impulse approximation (Commins and Bucksbaum [41]), and treat the nucleus as a collection of free independent nucleons. This justifies writing $\hat{J}_{\text{nuc } \mu}^{jn}$ as a sum of single nucleon operators, with each term, $\hat{J}_{\text{nuc } \mu}^{jn}$, given by [e.g., Weinberg [42], Eq. (2.20)]

$$\hat{J}_{\text{nuc } \mu}^{jn} = \hat{J}_{3\mu}^{jn} - \sin^2 \theta_W \hat{J}_{\text{EM}\mu}^{jn}, \quad (\text{A4})$$

where $\hat{J}_{3\mu}$ is the third component of the isovector current operator of β decay, and $\hat{J}_{\text{EM}\mu}$ is the electric current operator. In the low-energy limit, $\hat{J}_{\text{nuc } \mu}^{jn}$ is given by

$$\hat{J}_{\text{nuc } \mu}^{jn} = \gamma_\mu^{jn} [C_{V0} I^{jn} + \frac{1}{2} C_{V1} \tau_3^{jn} - \gamma_5^{jn} (C_{A0} I^{jn} + \frac{1}{2} C_{A1} \tau_3^{jn})], \quad (\text{A5})$$

where I^{jn} and τ_3^{jn} are the identity and third component of isospin operators in the neutron-proton isospin space. The form factors C_{V0} , C_{V1} , C_{A0} , C_{A1} in the $q=0$ ($q = |\bar{q}|$) limit are given in the standard model by

$$C_{V0} = -\sin^2 \theta_W, \quad C_{V1} = g_V - 2 \sin^2 \theta_W, \quad C_{A0} = 0, \\ C_{A1} = g_A, \quad (\text{A6})$$

with $g_V=1$, $g_A=1.23$, and $\sin^2\theta_W=0.23$. The j summation in Eq. (A2) is over all nucleons in a given nucleus, and the n summation is over the N_{nuc} nuclei in the scattering medium.

Analogous to the adiabatic or Born-Oppenheimer approximation used in condensed matter physics (e.g., Seitz [43]), we will assume that the nuclei are sufficiently far apart that the nucleons in a given nucleus are not significantly affected by the presence of other nuclei. We therefore assume that the state of the scattering medium can be decomposed into a product of states describing each nucleus and a

state describing the spatial correlations among the nuclei, i.e.,

$$\Psi(\bar{r}_{11}, \dots, \bar{r}_{AN_{\text{nuc}}}) = \psi(\bar{R}_1, \dots, \bar{R}_{N_{\text{nuc}}}) \phi_1(\bar{r}'_{11}, \dots, \bar{r}'_{A1}) \cdots \phi_{N_{\text{nuc}}}(\bar{r}'_{1N_{\text{nuc}}}, \dots, \bar{r}'_{AN_{\text{nuc}}}), \quad (\text{A7})$$

where \bar{R}_n locates the center of mass of the n th nucleus, and $\bar{r}'_{jn} = \bar{r}_{jn} - \bar{R}_n$ locates the position of the j th nucleon of the n th nucleus relative to the latter's center of mass. Substituting Eq. (A7) into Eq. (A2) gives

$$\begin{aligned} M &= \frac{GL^\mu}{\sqrt{2}} \sum_{n=1}^{N_{\text{nuc}}} \langle \psi_f | \exp[(i/\hbar)\bar{q} \cdot \bar{R}_n] | \psi_i \rangle \left\langle \phi_{f1} \cdots \phi_{fN_{\text{nuc}}} \left| \sum_{j=1}^A \hat{J}_{\text{nuc}\mu}^j \exp[(i/\hbar)\bar{q} \cdot \bar{r}'_{jn}] \right| \phi_{i1} \cdots \phi_{iN_{\text{nuc}}} \right\rangle \\ &= \frac{GL^\mu}{\sqrt{2}} \sum_{n=1}^{N_{\text{nuc}}} \langle \psi_f | \exp[(i/\hbar)\bar{q} \cdot \bar{R}_n] | \psi_i \rangle \left\langle \phi_{fn} \left| \sum_{j=1}^A \hat{J}_{\text{nuc}\mu}^j \exp[(i/\hbar)\bar{q} \cdot \bar{r}'_{jn}] \right| \phi_{in} \right\rangle \\ &= \frac{GL^\mu}{\sqrt{2}} \left\langle \psi_f \left| \sum_{n=1}^{N_{\text{nuc}}} \exp[(i/\hbar)\bar{q} \cdot \bar{R}_n] \right| \psi_i \right\rangle \left\langle \phi_f \left| \sum_{j=1}^A \hat{J}_{\text{nuc}\mu}^j \exp[(i/\hbar)\bar{q} \cdot \bar{r}'_j] \right| \phi_i \right\rangle, \end{aligned} \quad (\text{A8})$$

where in the last step we have assumed that $\phi_{f1} = \phi_{f2} = \cdots = \phi_{fN} = \phi_f$ and $\phi_{i1} = \phi_{i2} = \cdots = \phi_{iN} = \phi_i$, i.e., that all nuclei are identical, and we have dropped the subscripts n because the expectation value of the operator should be independent of which nucleus is being considered.

We now take the implied sum over the neutrino spins in the modulus squared to get

$$\begin{aligned} \sum_{\text{spins}} L^\alpha L^{*\beta} &= \frac{2c^2}{V^2 E_{\nu f} E_{\nu i}} [p_{\nu f}^\alpha p_{\nu i}^\beta - g^{\alpha\beta} (p_{\nu f} \cdot p_{\nu i}) + p_{\nu f}^\beta p_{\nu i}^\alpha \\ &\quad - i p_{\nu f \sigma} p_{\nu i \tau} \epsilon^{\sigma\alpha\tau\beta}], \end{aligned} \quad (\text{A9})$$

Denoting $\langle \phi_f | \sum_{j=1}^A \hat{J}_{\text{nuc}\mu}^j \exp[(i/\hbar)\bar{q} \cdot \bar{r}'_j] | \phi_i \rangle$ by $\langle J_{\text{nuc}\mu} \rangle$, we perform the inner product of the lepton currents $L^\alpha L^{*\beta}$ and the nuclear currents $\langle J_{\text{nuc}\alpha} \rangle \langle J_{\text{nuc}\beta} \rangle^*$, and then take the average over the angle appearing in the spatial component of the inner product, which is equivalent to averaging over the nuclear spin projection; we obtain

$$\begin{aligned} w_{fi} &= \frac{2\pi}{\hbar} \delta(E_{\text{nuc}f} - E_{\text{nuc}i} + E_{\nu f} - E_{\nu i}) \frac{G^2}{V^2} \\ &\quad \times \{ |\langle J_{\text{nuc}}^0 \rangle|^2 [1 + \hat{\mathbf{p}}_{\nu f} \cdot \hat{\mathbf{p}}_{\nu i}] + |\langle \bar{J}_{\text{nuc}} \rangle|^2 [1 - \frac{1}{3} \hat{\mathbf{p}}_{\nu f} \cdot \hat{\mathbf{p}}_{\nu i}] \} \\ &\quad \times \left| \left\langle \psi_f \left| \sum_{n=1}^{N_{\text{nuc}}} \exp[(i/\hbar)\bar{q} \cdot \bar{R}_n] \right| \psi_i \right\rangle \right|^2, \end{aligned} \quad (\text{A10})$$

where J_{nuc}^0 and \bar{J}_{nuc} are the time and space components of the nuclear 4-current, and $\hat{\mathbf{p}}_{\nu f}$ and $\hat{\mathbf{p}}_{\nu i}$ are unit vectors in the direction of the final and initial neutrino momenta, respectively; i.e., $\hat{\mathbf{p}}_{\nu f} = c\bar{p}_{\nu f}/E_{\nu f}$ and $\hat{\mathbf{p}}_{\nu i} = c\bar{p}_{\nu i}/E_{\nu i}$. Note that the cross terms in Eq. (A10) vanish as a result of the spin projection averaging.

The nonrelativistic approximation is appropriate for nucleons in the nucleus. In this approximation, the small components of the nucleon spinors, which are $O(v/c)$, are neglected; the spinor operators in Eq. (A4) assume the limits $\gamma^0 \rightarrow I$, $\gamma^0 \gamma^5 \rightarrow 0$, $\gamma^i \rightarrow 0$, and $\gamma^i \gamma^5 \rightarrow \sigma_i$. Then $\langle J_{\text{nuc}}^0 \rangle$ and $\langle \bar{J}_{\text{nuc}} \rangle$ become

$$\langle J_{\text{nuc}}^0 \rangle = \left\langle \phi_f \left| \sum_{j=1}^A (C_{V0} I^j + \frac{1}{2} C_{V1} \tau_3^j) \exp[(i/\hbar)\bar{q} \cdot \bar{r}'_j] \right| \phi_i \right\rangle, \quad (\text{A11})$$

and

$$\langle \bar{J}_{\text{nuc}} \rangle = - \left\langle \phi_f \left| \sum_{j=1}^A (C_{A0} I^j + \frac{1}{2} C_{A1} \tau_3^j) \bar{\sigma} \exp[(i/\hbar)\bar{q} \cdot \bar{r}'_j] \right| \phi_i \right\rangle. \quad (\text{A12})$$

To evaluate $|\langle J_{\text{nuc}}^0 \rangle|^2$ and $|\langle \bar{J}_{\text{nuc}} \rangle|^2$ in Eq. (A10), we assume that the scattering is elastic, i.e., that the nuclear state $|\phi_i\rangle$ does not change as a result of the scattering. The nuclear recoil will be incorporated in $|\psi_f\rangle$. Consider first Eq. (A11) for $\langle J_{\text{nuc}}^0 \rangle$. We rewrite this equation in terms of the proton and neutron ‘‘projection’’ operators $\xi_p^j = \frac{1}{2}(I^j + \tau_3^j)$ and $\xi_n^j = \frac{1}{2}(I^j - \tau_3^j)$ —i.e., $\xi_{p(n)}^j |\phi_i\rangle = |\phi_i\rangle$ for protons (neutrons), and zero otherwise—to get

$$\begin{aligned} \langle J_{\text{nuc}}^0 \rangle &= \left\langle \phi_i \left| \sum_{j=1}^A (C_{Vp} \xi_p^j + C_{Vn} \xi_n^j) \exp[(i/\hbar)\bar{q} \cdot \bar{r}'_j] \right| \phi_i \right\rangle \\ &= C_{Vp} \left\langle \phi_i \left| \sum_{\text{protons}} \exp[(i/\hbar)\bar{q} \cdot \bar{r}'_j] \right| \phi_i \right\rangle \\ &\quad + C_{Vn} \left\langle \phi_i \left| \sum_{\text{neutrons}} \exp[(i/\hbar)\bar{q} \cdot \bar{r}'_j] \right| \phi_i \right\rangle \\ &= C_{Vp} Z F_p(\bar{q}) + C_{Vn} N F_n(\bar{q}), \end{aligned} \quad (\text{A13})$$

where $C_{Vp} = C_{V0} + \frac{1}{2}C_{V1}$ and $C_{Vn} = C_{V0} - \frac{1}{2}C_{V1}$, and where

$$\begin{aligned} ZF_p(\vec{q}) &= \left\langle \phi_i \left| \sum_{\text{protons}} \exp[(i/\hbar)\vec{q} \cdot \vec{r}'_j] \right| \phi_i \right\rangle, \\ NF_n(\vec{q}) &= \left\langle \phi_i \left| \sum_{\text{neutrons}} \exp[(i/\hbar)\vec{q} \cdot \vec{r}'_j] \right| \phi_i \right\rangle. \end{aligned} \quad (\text{A14})$$

$F_p(\vec{q})$ and $F_n(\vec{q})$ are the proton and neutron form factors for the composite nuclear target. Both are simply the superposition of unit amplitudes with phase factors that account for the relative phases of the scattering from the individual protons and neutrons in the nucleus, each at a different coordinate \vec{r}'_j . Expressions for the form factors in terms of nuclear parameters can be obtained by considering their Fourier transforms. Thus

$$\begin{aligned} &\frac{1}{(2\pi\hbar)^3} \int d^3\vec{q} \exp[-(i/\hbar)\vec{q} \cdot \vec{r}] F_p(\vec{q}) \\ &= \frac{1}{Z(2\pi\hbar)^3} \int d^3\vec{q} \exp[-(i/\hbar)\vec{q} \cdot \vec{r}] \\ &\quad \times \left\langle \phi_i^p \left| \sum_{\text{protons}} \exp[(i\hbar)\vec{q} \cdot \vec{r}'_j] \right| \phi_i^p \right\rangle \\ &= \frac{1}{Z} \left\langle \phi_i^p \left| \sum_{\text{protons}} \delta^3(\vec{r} - \vec{r}'_j) \right| \phi_i^p \right\rangle = \rho_p(\vec{r}), \end{aligned} \quad (\text{A15})$$

where $\rho_p(\vec{r})$ is the normalized proton density in the nucleus. It therefore follows that $F_p(\vec{q})$ is the Fourier transform of $\rho_p(\vec{r})$. By the same argument, $F_n(\vec{q})$ is the Fourier transform of $\rho_n(\vec{r})$, the normalized neutron density in the nucleus. We will assume that

$$F_p(\vec{q}) = F_n(\vec{q}) = F(\vec{q}). \quad (\text{A16})$$

While the best fit to the proton distribution, based on electron scattering data, is the two-parameter ‘‘Fermi-Dirac’’ distribution (Hofstadter [44]), an approximation for $\rho(\vec{r})$ that correctly reproduces the nuclear mean square radius and permits closed form expressions for the final scattering rates is the Gaussian

$$\rho(\vec{r}) = \frac{1}{\left(\frac{2}{3}\pi\langle r^2 \rangle\right)^{3/2}} \exp[-(3/2)(r^2/\langle r^2 \rangle)] \quad (\text{A17})$$

for which

$$F(\vec{q}) = \exp(-b|\vec{q}|^2), \quad (\text{A18})$$

where $b = (1/\hbar^2)(r^2/6)$, and $|\vec{q}|^2 = 2p_{\nu f} \cdot p_{\nu i} = 2(\epsilon_\nu^2/c^2)(1 - \cos \theta)$, where $\theta = \cos^{-1} \hat{\mathbf{p}}_{\nu f} \cdot \hat{\mathbf{p}}_{\nu i}$ is the scattering angle (i.e., the angle of the final neutrino momentum relative to the initial neutrino momentum). The result for $\langle J_{\text{nuc}}^0 \rangle$ from Eqs. (A13) and (A18) is

$$\langle J_{\text{nuc}}^0 \rangle = \left(C_{V0}A + C_{V1} \frac{Z-N}{2} \right) \exp[-2b(\epsilon_\nu^2/c^2)(1 - \cos \theta)]. \quad (\text{A19})$$

Now consider $\langle \bar{J}_{\text{nuc}} \rangle$ given by Eq. (A12). This part of the matrix element is usually neglected in comparison with $\langle J_{\text{nuc}}^0 \rangle$. The basic reason is that spin is the additive quantum number for axial vector coupling, and the final cross section is proportional to $J(J+1)$, where J is the nuclear spin of the target. This is unlike the vector coupling case, where baryon number is the additive quantum number. Since $J(J+1) \ll A^2$, coherent effects are minimal for axial vector coupling. Additionally, the coefficient C_{A0} is zero in the standard model, and C_{A1} will vanish for $J=0$ (ground state) nuclei. For these reasons we have set the contribution of $\langle \bar{J}_{\text{nuc}} \rangle$ to the neutrino-nucleus scattering rate to zero in our supernova code.

Using Eq. (A19) in Eq. (A10), and setting $\langle \bar{J}_{\text{nuc}} \rangle$ to zero, we obtain

$$\begin{aligned} w_{fi} &= \frac{2\pi}{\hbar} \delta(E_{\text{nuc}f} - E_{\text{nuc}i} + E_{\nu f} - E_{\nu i}) \frac{C^2}{V^2} (1 + \cos \theta) \\ &\quad \times \exp[-4b(E_\nu^2/c^2)(1 - \cos \theta)] \\ &\quad \times \left\langle \left| \psi_f \left| \sum_{n=1}^{N_{\text{nuc}}} \exp[(i/\hbar)\vec{q} \cdot \vec{R}_n] \right| \psi_i \right| \right\rangle^2, \end{aligned} \quad (\text{A20})$$

where

$$C^2 = G^2 A^2 \left| C_{V0} + C_{V1} \frac{Z-N}{2A} \right|^2. \quad (\text{A21})$$

The effect of the nuclear form factor

$$F^2(q) = \exp[-4b(E_\nu^2/c^2)(1 - \cos \theta)] \quad (\text{A22})$$

in Eq. (A20) is to reduce the transition rate at high neutrino energies. This reduction will occur, for a given scattering angle θ , when the amplitudes for scattering from the various nucleons in a nucleus interfere destructively with each other. (This occurs at high enough neutrino energy, when the neutrino wavelength becomes comparable to the nuclear radius. Complete destructive interference occurs when the path difference between neutrino scattering on two separate nucleons is one-half the neutrino wavelength.) To estimate this effect, take the nuclear radius to be $R = 1.07A^{1/3}$ fm. Note that the mean scattering angle in the absence of the correction factors, Eq. (A22) and the term in Eq. (A20) that corresponds to Eq. (A24), is $\theta = 3\pi/8$. For this scattering angle and for $A = 56$, we find that the nuclear form factor reduces the transition rate by a factor e^{-1} when $E_\nu = 83$ MeV, and for $A = 100$, by the same factor when $E_\nu = 68$ MeV. These neutrino energies are too high for the neutrino opacities to be affected near the neutrinosphere, but during core infall the ν_e chemical potential reaches 68 MeV at $\rho \approx 2 \times 10^{13}$ g cm $^{-3}$; therefore the nuclear form factors will reduce the neutrino opacities at these higher densities, and therefore increase the rate of neutrino transport in the dense inner part of the core.

The neutrino-nucleus scattering source terms in the supernova code are functions of $R_{\nu-A}$, the neutrino-nucleus scattering kernel. The latter is the scattering rate for a given initial and final neutrino state, and is obtained by summing and averaging w_{fi} over final and initial nuclear states, respectively, i.e.,

$$\begin{aligned}
R_{\nu-A} &= \sum_{\text{nuc } i} \sum_{\text{nuc } f} P_{\text{nuc } i} W_{fi} \\
&\equiv \frac{2\pi}{\hbar} C^2 (1 + \cos\theta) \exp[-4b(E_\nu^2/c^2)(1 - \cos\theta)] \\
&\quad \times \frac{N_{\text{nuc}}}{V^2} \mathcal{S}_{\text{ion}}(\Delta E_\nu, \bar{q}), \tag{A23}
\end{aligned}$$

where $\Delta E_\nu = E_{\nu f} - E_{\nu i}$ is the energy transferred from the neutrino to the medium. Here $P_{\text{nuc } i}$ is the probability of a given initial state, and the average is taken over the canonical ensemble at temperature T . Note that $\sum_{\text{nuc } i, f}$ are symbolic sums taken over all initial and final states $\psi_{i, f}$ of the correlated nuclei centers of mass. $\mathcal{S}_{\text{ion}}(\Delta E_\nu, \bar{q})$ is referred to as the ‘‘dynamic structure function’’ or ‘‘dynamic form factor’’ of the medium (e.g., Van Hove [45], Pines and Nozières [46], Hansen and McDonald [47]), and is given by

$$\begin{aligned}
\mathcal{S}_{\text{ion}}(\Delta E_\nu, \bar{q}) &= \frac{1}{N_{\text{nuc}}} \sum_{\text{nuc } i} \sum_{\text{nuc } f} P_{\text{nuc } i} \left| \left\langle \psi_f \left| \sum_{n=1}^{N_{\text{nuc}}} \exp[(i/\hbar)\bar{q} \cdot \bar{R}_n] \right| \psi_i \right\rangle \right|^2 \\
&\quad \times \delta(E_{\text{nuc } f} - E_{\text{nuc } i} - \Delta E_\nu). \tag{A24}
\end{aligned}$$

An important simplification can be made considering the fact that the recoil energy of the nucleus is very small. In particular, the δ function in Eq. (A24) can be written as

$$\begin{aligned}
\delta(E_{\text{nuc } f} - E_{\text{nuc } i} - \Delta E_\nu) &= \delta\left(\frac{\bar{q} \cdot \bar{P}_{\text{nuc}}}{M_{\text{nuc}}} + \frac{|\bar{q}|^2}{2M_{\text{nuc}}} - \Delta E_\nu\right) \\
&\simeq \delta\left(\frac{\bar{q} \cdot \bar{P}_{\text{nuc}}}{M_{\text{nuc}}} - \Delta E_\nu\right), \tag{A25}
\end{aligned}$$

where we have used the fact that $|\bar{P}_{\text{nuc}}|c \simeq \sqrt{3M_{\text{nuc}}c^2kT} > |\bar{q}|c \sim E_\nu$, unless $E_{\text{Fermi}}/kT > 55$, where E_{Fermi} is the electron Fermi energy. During collapse, $E_{\text{Fermi}}/kT < 20$. Since $|\bar{q}|c \leq 2E_{\nu i}$, we have

$$\frac{\bar{q} \cdot \bar{P}_{\text{nuc}}}{M_{\text{nuc}}} = \bar{q} \cdot \bar{V}_{\text{nuc}} \leq 2E_{\nu i} \frac{\bar{V}_{\text{nuc}}}{c} \ll E_{\nu i}. \tag{A26}$$

It follows from Eqs. (A26) and (A25) that $\Delta E_\nu \ll E_{\nu i}$ for any scattering angle. Hence, a good approximation is to assume that $\Delta E_\nu = 0$ for all scatterings and write

$$\mathcal{S}_{\text{ion}}(\Delta E_\nu, \bar{q}) \equiv \delta(\Delta E_\nu) \mathcal{S}_{\text{ion}}(\bar{q}), \tag{A27}$$

where

$$\mathcal{S}_{\text{ion}}(\bar{q}) \equiv \int_{-\infty}^{\infty} d\Delta E_\nu \mathcal{S}_{\text{ion}}(\Delta E_\nu, \bar{q}). \tag{A28}$$

Here $\mathcal{S}_{\text{ion}}(\bar{q})$ is referred to as the ‘‘static structure function’’ or ‘‘static form factor’’ of the medium [‘‘static,’’ as will be seen below, because the times in the arguments of \bar{R}_m and \bar{R}_n in Eq. (A30) become equal]. In the context of stellar core collapse, $\mathcal{S}_{\text{ion}}(\bar{q})$ is referred to as the ‘‘ion screening factor’’ or ‘‘ion screening correction.’’ With Eq. (A27), Eq. (A23) becomes

$$\begin{aligned}
R_{\nu-A} &= \frac{2\pi}{\hbar} C^2 (1 + \cos\theta) \exp[-4b(E_\nu^2/c^2)(1 - \cos\theta)] \\
&\quad \times \frac{N_{\text{nuc}}}{V^2} \delta(E_{\nu f} - E_{\nu i}) \mathcal{S}_{\text{ion}}(\bar{q}). \tag{A29}
\end{aligned}$$

To further explore the properties of $\mathcal{S}_{\text{ion}}(\bar{q})$, we transform Eq. (A24) into a more convenient form by inserting the Fourier representation of the δ function to get

$$\begin{aligned}
\mathcal{S}_{\text{ion}}(\Delta E_\nu, \bar{q}) &= \frac{1}{N_{\text{nuc}}} \sum_{\text{nuc } i} \sum_{\text{nuc } f} P_{\text{nuc } i} \frac{1}{2\pi\hbar} \int_{-\infty}^{\infty} dt \exp\left(\frac{i}{\hbar}(E_{\text{nuc } f} - E_{\text{nuc } i} - \Delta E_\nu)t\right) \left| \left\langle \psi_f \left| \sum_{n=1}^{N_{\text{nuc}}} \exp\left(\frac{i}{\hbar}\bar{q} \cdot \bar{R}_n\right) \right| \psi_i \right\rangle \right|^2 \\
&= \frac{1}{N_{\text{nuc}}} \sum_{\text{nuc } i} \sum_{\text{nuc } f} P_{\text{nuc } i} \frac{1}{2\pi\hbar} \int_{-\infty}^{\infty} dt \exp[(-i/\hbar)t\Delta E_\nu] \left\langle \psi_i \left| \sum_{n=1}^{N_{\text{nuc}}} \exp[(-i\hbar)\bar{q} \cdot \bar{R}_n] \right| \psi_f \right\rangle \\
&\quad \times \left\langle \psi_f \left| \exp[(i/\hbar)\hat{H}t] \sum_{m=1}^{N_{\text{nuc}}} \exp[(i/\hbar)\bar{q} \cdot \bar{R}_m] \exp[-(i/\hbar)\hat{H}t] \right| \psi_i \right\rangle \\
&= \frac{1}{N_{\text{nuc}}} \sum_{\text{nuc } i} P_{\text{nuc } i} \sum_{n=1}^{N_{\text{nuc}}} \sum_{m=1}^{N_{\text{nuc}}} \frac{1}{2\pi\hbar} \int_{-\infty}^{\infty} dt \exp[(-i/\hbar)t\Delta E_\nu] \langle \psi_i | \exp[-(i/\hbar)\bar{q} \cdot \bar{R}_n(0)] \exp[(i/\hbar)\bar{q} \cdot \bar{R}_m(t)] | \psi_i \rangle \\
&\equiv \frac{1}{N_{\text{nuc}}} \sum_{n=1}^{N_{\text{nuc}}} \sum_{m=1}^{N_{\text{nuc}}} \frac{1}{2\pi\hbar} \int_{-\infty}^{\infty} dt \exp[(-i/\hbar)t\Delta E_\nu] \langle \exp[-(i/\hbar)\bar{q} \cdot \bar{R}_n(0)] \exp[(i/\hbar)\bar{q} \cdot \bar{R}_m(t)] \rangle, \tag{A30}
\end{aligned}$$

where \hat{H} is the Hamiltonian for the correlated nuclei centers of mass, and where, using the time-translation property of \hat{H} , we have defined $\bar{R}_n(0) = \bar{R}_n$, $\bar{R}_m(t) = \exp[(i/\hbar)\hat{H}t]\bar{R}_m\exp[-(i/\hbar)\hat{H}t]$. The sum over final states has been performed by exploiting the closure property ($\sum |\psi_f\rangle\langle\psi_f| = 1$) of a complete set of quantum states $|\psi_f\rangle$, and we have denoted the combination of quantum and canonical statistical averaging by $\langle \cdot \rangle$. We then use Eq. (A30) for $\mathcal{S}_{\text{ion}}(\Delta E_\nu, \bar{q})$ and carry out the integration over ΔE_ν :

$$\begin{aligned}
\mathcal{S}_{\text{ion}}(\bar{q}) &= \int_{-\infty}^{\infty} d\Delta E_{\nu} \mathcal{S}_{\text{ion}}(\Delta E_{\nu}, \bar{q}) \\
&= \frac{1}{N_{\text{nuc}}} \sum_{n=1}^{N_{\text{nuc}}} \sum_{m=1}^{N_{\text{nuc}}} \int_{-\infty}^{\infty} dt \delta(t) \\
&\quad \times \langle \exp[-(i/\hbar)\bar{q} \cdot \bar{R}_n(0)] \exp[(i/\hbar)\bar{q} \cdot \bar{R}_m(t)] \rangle \\
&= \frac{1}{N_{\text{nuc}}} \sum_{n=1}^{N_{\text{nuc}}} \sum_{m=1}^{N_{\text{nuc}}} \langle \exp[-(i/\hbar)\bar{q} \cdot \bar{R}_n] \\
&\quad \times \exp[(i/\hbar)\bar{q} \cdot \bar{R}_m] \rangle \\
&= \frac{1}{N_{\text{nuc}}} \sum_{n=1}^{N_{\text{nuc}}} \sum_{m=1}^{N_{\text{nuc}}} \langle \exp[-(i/\hbar)\bar{q} \cdot \bar{R}_n] \\
&\quad \times \exp[(i/\hbar)\bar{q} \cdot \bar{R}_m] \rangle. \tag{A31}
\end{aligned}$$

Because the position operators \bar{R}_n and \bar{R}_m are now at equal times, they commute, and further instructive transformations of $\mathcal{S}_{\text{ion}}(\bar{q})$ are possible:

$$\begin{aligned}
\mathcal{S}_{\text{ion}}(\bar{q}) &= \frac{1}{N_{\text{nuc}}} \sum_{n=1}^{N_{\text{nuc}}} \sum_{m=1}^{N_{\text{nuc}}} \langle \exp[\\
&\quad -(i/\hbar)\bar{q} \cdot \bar{R}_n] \exp[(i/\hbar)\bar{q} \cdot \bar{R}_m] \rangle \\
&= 1 + \frac{1}{N_{\text{nuc}}} \sum_{n \neq m}^{N_{\text{nuc}}} \left\langle \int \int d^3\bar{r} d^3\bar{r}' \right. \\
&\quad \left. \times \exp[-(i/\hbar)\bar{q} \cdot (\bar{r} - \bar{r}')] \delta(\bar{r} - \bar{R}_n) \delta(\bar{r}' - \bar{R}_m) \right\rangle \\
&\equiv 1 + \frac{1}{N_{\text{nuc}}} \frac{N_{\text{nuc}}(N_{\text{nuc}} - 1)}{V^2} \int \int d^3\bar{r} d^3\bar{r}' \\
&\quad \times \exp[-(i/\hbar)\bar{q} \cdot (\bar{r} - \bar{r}')] g(\bar{r} - \bar{r}') \\
&\approx 1 + n_{\text{nuc}} \int d^3\bar{r} \exp[-(i/\hbar)\bar{q} \cdot \bar{r}] g(\bar{r}) \\
&= 1 + n_{\text{nuc}} (2\pi\hbar)^3 \delta^3(\bar{q}) + n_{\text{nuc}} \int d^3\bar{R} \\
&\quad \times \exp[-(i/\hbar)\bar{q} \cdot \bar{R}] [g(\bar{R}) - 1], \tag{A32}
\end{aligned}$$

where $n_{\text{nuc}} = N_{\text{nuc}}/V$ is the number density of nuclei. In the fourth equality we have assumed that $N_{\text{nuc}} - 1 \approx N_{\text{nuc}}$. To establish the last equality unity has been added and subtracted to the integrand, and the unimportant scattering term at $\bar{q} = \bar{0}$ has been factored out. We will ignore this term in what follows. The quantity $g(\bar{R})$ is the pair distribution function, defined as

$$\begin{aligned}
g(\bar{R}_1, \bar{R}_2) &= V^2 \langle \bar{R}'_1, \bar{R}'_2 | \delta^3(\bar{R}_1 - \bar{R}'_1) \delta^3(\bar{R}_2 - \bar{R}'_2) | \bar{R}'_1, \bar{R}'_2 \rangle \\
&= g(\bar{R}_1 - \bar{R}_2) \tag{A33}
\end{aligned}$$

[47], where the last equality in Eq. (A32) holds for a translationally invariant system.

The pair distribution function gives the probability of finding another nucleus at a position \bar{R} from a given nucleus relative to that probability if the positions of the nuclei were completely uncorrelated. If the positions of the nuclei are completely uncorrelated, $g(\bar{R}) = 1$, and the expression given in the last line of Eq. (A31) shows that $\mathcal{S}_{\text{ion}} = 1$. In this case, ion screening has no effect. In the extreme opposite case, which occurs when $T = 0$, the canonical ensemble consists of just the ground state, in which the nuclei are arranged in a rigid lattice. If in addition the scattering leaves the nuclei in the ground state, i.e., $|\psi_f\rangle = |\psi_i\rangle$, then \mathcal{S}_{ion} as given by Eq. (A24) becomes identical in form to the square of the proton and neutron nuclear form factors, given by Eq. (A13). In this case, \mathcal{S}_{ion} will be directly related to the Fourier transform of the distribution of nuclei, and the neutrino scattering will be analogous to the Bragg scattering of x rays in a crystal. In particular, the scattering will be zero if the neutrino momentum is below a minimum value corresponding to a wavelength greater than twice the spacing between adjacent planes of the lattice. In the intermediate ‘‘liquid’’ case, $g(\bar{R}) = g(|\bar{R}|)$, i.e., the pair distribution will be isotropic, and its magnitude will be characterized by a peak at the nearest neighbor distance a , with $g(|\bar{R}|) \rightarrow 0$ as $|\bar{R}| \rightarrow 0$ and $g(|\bar{R}|) \rightarrow 1$ as $|\bar{R}| \rightarrow \infty$. In this case, \mathcal{S}_{ion} must be computed numerically, but has a similar appearance, with a peak at a value of $|\bar{q}|$ approximately equal to $2\pi/a$ (e.g., Hansen and McDonald [47], Fig. 11), and small when $|\bar{q}| \rightarrow 0$.

We now use Eq. (A29) to obtain the source terms needed for our supernova code. Assuming spherical symmetry, let $f = f(t, r, E_{\nu}, \mu)$ be the neutrino occupation number, i.e., the number of neutrinos per state, where t is the time, r is the radial distance from the core center, E_{ν} is the neutrino energy, and μ is the cosine of the angle of the neutrino propagation direction with respect to the outward radial direction. Then

$$dn_{\nu} = f(t, r, E_{\nu}, \mu) \frac{2\pi dV E_{\nu}^2 dE_{\nu} d\mu}{(2\pi\hbar c)^3}, \tag{A34}$$

where dn_{ν} is the number of neutrinos at (t, r, E_{ν}, μ) in $dV dE_{\nu} d\mu$. The neutrino transport equation equates the rate of change of f to appropriate flow and source terms. The contribution of neutrino-nucleus scattering to the transport equation is obtained by computing $B_{\nu-A}$, which is the rate at which neutrinos are scattered into the state at $(r, E_{\nu \text{ in}}, \mu_{\text{in}})$ minus the rate at which neutrinos are scattered out of that state. Factoring out the δ function from $R_{\nu-A}$ in Eq. (A29) by writing

$$R_{\nu-A} = \delta(E_{\nu f} - E_{\nu i}) R'_{\nu-A}, \tag{A35}$$

the equation for $B_{\nu-A}(t, r, E_{\nu \text{ in}}, \mu_{\text{in}})$ is given by

$$\begin{aligned}
B_{\nu-A} &= [1 - f_{\text{in}}] \frac{V}{(2\pi\hbar c)^3} \int_0^\infty E_{\nu \text{ out}}^2 dE_{\nu \text{ out}} \int_{-1}^1 d\mu_{\text{out}} \\
&\times \int_0^{2\pi} d\phi_{\text{out}} f_{\text{out}} \delta(E_{\nu \text{ out}} - E_{\nu \text{ in}}) R'_{\nu-A} \\
&- f_{\text{in}} \frac{V}{(2\pi\hbar c)^3} \int_0^\infty E_{\nu \text{ out}}^2 dE_{\nu \text{ out}} \int_{-1}^1 d\mu_{\text{out}} \\
&\times \int_0^{2\pi} d\phi_{\text{out}} [1 - f_{\text{out}}] \delta(E_{\nu \text{ out}} - E_{\nu}) R'_{\nu-A} \\
&= \frac{VE_{\nu \text{ in}}^2}{(2\pi\hbar c)^3} \int_{-1}^1 d\mu_{\text{out}} \int_0^{2\pi} d\phi_{\text{out}} R'_{\nu-A} [f_{\text{out}} - f_{\text{in}}],
\end{aligned} \tag{A36}$$

where $f_{\text{in}} = f(t, r, E_{\nu \text{ in}}, \mu_{\text{in}})$, $f_{\text{out}} = f(t, r, E_{\nu \text{ out}}, \mu_{\text{out}})$, and $R'_{\nu-A} = R'_{\nu-A}(t, r, E_{\nu \text{ in}}, \cos \theta)$, with

$$\cos \theta = \mu_{\text{in}} \mu_{\text{out}} + \sqrt{(1 - \mu_{\text{in}}^2)(1 - \mu_{\text{out}}^2)} \cos(\phi_{\text{out}} - \phi_{\text{in}}). \tag{A37}$$

In the multigroup flux-limited diffusion (MGFLD) scheme, which is the scheme implemented in our supernova code, we solve for the zeroth ($\psi^{(0)}$) and first ($\psi^{(1)}$) moments of the neutrino distribution function f ; the n th moment, $\psi^{(n)}$, is defined by

$$\psi^{(n)} \equiv \frac{1}{2} \int_{-1}^1 \mu^n d\mu f, \tag{A38}$$

where, in accordance with our assumption of spherical symmetry, azimuthal symmetry about the radial direction has been assumed. The MGFLD equations for $\psi^{(0)}$ and $\psi^{(1)}$ are

$$\frac{1}{c} \frac{\partial \psi^{(0)}}{\partial t} + \frac{1}{r^2} \frac{\partial (r^2 \psi^{(1)})}{\partial r} + \text{velocity terms} = \text{RHS}^{(0)} \tag{A39}$$

and

$$\psi^{(1)} = -\frac{\lambda^t}{3} \mathcal{F} \frac{\partial \psi^{(0)}}{\partial r}, \tag{A40}$$

where the diffusion coefficient λ^t is given by

$$\lambda^t \equiv \frac{\psi^{(0)}}{\text{RHS}^{(0)} - \text{rhs}^{(1)}} \tag{A41}$$

where $\text{RHS} = B_{\nu-A} + \text{other processes}$, and where

$$\text{RHS}^{(n)} \equiv \frac{1}{2} \int_{-1}^1 \mu^n d\mu \text{RHS}, \tag{A42}$$

$\text{rhs}^{(1)} = \text{RHS}^{(1)} \psi^{(0)} / \psi^{(1)}$, and \mathcal{F} is the ‘‘flux limiter,’’ a parameter constructed to keep the flux from becoming unphysically large when λ^t becomes large. Therefore it is the zeroth and first angular moments of $B_{\nu-A}$ that are needed, which we denote by $B_{\nu-A}^{(0)}$ and $B_{\nu-A}^{(1)}$, respectively.

To obtain closed form expressions for these angular moments, we expand $R'_{\nu-A}$ in the first two terms of a Legendre series:

$$\begin{aligned}
R'_{\nu-A}(t, r, E_{\nu}, \cos \theta) &= \frac{1}{2} \Phi_{0\nu-A}(t, r, E_{\nu}) \\
&+ \frac{3}{2} \Phi_{1\nu-A}(t, r, E_{\nu}) \cos \theta.
\end{aligned} \tag{A43}$$

Then, using Eqs. (A43) and (A37) in Eq. (A36), we obtain

$$B_{\nu-A}^{(0)} \equiv \frac{1}{2} \int_{-1}^1 d\mu_{\text{in}} B_{\nu-A} = 0, \tag{A44}$$

$$\begin{aligned}
B_{\nu-A}^{(1)} &\equiv \frac{1}{2} \int_{-1}^1 \mu_{\text{in}} d\mu_{\text{in}} B_{\nu-A} \\
&= 2\pi \frac{VE_{\nu \text{ in}}^2}{(2\pi\hbar c)^3} [\Phi_{1\nu-A} - \Phi_{0\nu-A}] \psi^{(1)}.
\end{aligned} \tag{A45}$$

Equation (A44) states that neutrino-nucleus isoenergetic scattering gives no contribution to the source of $\psi^{(0)}$. This is because neutrino-nucleus isoenergetic scattering redistributes the neutrinos in angle only, and therefore gives zero contribution in the angle average. The negative of the coefficient of $\psi^{(1)}$ in Eq. (A45) is the neutrino-nucleus isoenergetic scattering contribution to the inverse transport mean free path, which is used in the MGFLD scheme to relate $\psi^{(1)}$ to the radial gradient of $\psi^{(0)}$ [e.g., Bruenn [9], Eqs. (A26) and (A41)].

To obtain explicit expressions for $\Phi_{0\nu-A}$ and $\Phi_{1\nu-A}$, we observe that the expression for $\langle \mathcal{S}_{\text{ion}} \rangle$ provided by Horowitz is defined by

$$\langle \mathcal{S}_{\text{ion}} \rangle = \frac{3}{4} \int_{-1}^1 d \cos \theta (1 + \cos \theta) (1 - \cos \theta) \mathcal{S}_{\text{ion}}(\bar{q}). \tag{A46}$$

The factor $(1 - \cos \theta)$ is the appropriate ‘‘transport’’ angular weighting factor. To derive an expression for $\Phi_{0\nu-A} - \Phi_{1\nu-A}$, first ignore the nuclear form factor [Eq. (A22)], which is valid at low neutrino energies. Therefore $R'_{\nu-A}$, as given by Eqs. (A35) and (A29), becomes

$$R'_{\nu-A} = \frac{2\pi}{\hbar} n_{\text{nuc}} \frac{G^2}{V} A^2 \left| C_{V0} + C_{V1} \frac{Z-N}{2A} \right|^2 (1 + \cos \theta) \mathcal{S}_{\text{ion}}. \tag{A47}$$

Then, using Eqs. (A46) and (A47) and the definitions of $\Phi_{0\nu-A}$ and $\Phi_{1\nu-A}$, we obtain

$$\begin{aligned}
\Phi_{0\nu-A}^{\text{low}} - \Phi_{1\nu-A}^{\text{low}} &\equiv \int_{-1}^1 d \cos \theta (1 - \cos \theta) R'_{\nu-A} \\
&= \frac{2\pi}{\hbar} n_{\text{nuc}} \frac{G^2}{V} A^2 \left| C_{V0} + C_{V1} \frac{Z-N}{2A} \right|^2 \frac{4}{3} \langle \mathcal{S}_{\text{ion}} \rangle,
\end{aligned} \tag{A48}$$

where the superscript ‘‘low’’ is a reminder that this expression for $\Phi_{0\nu-A} - \Phi_{1\nu-A}$ is valid only at low neutrino energies.

For high neutrino energies we must include the nuclear form factor. In this case, set \mathcal{S}_{ion} equal to 1 in Eq. (A23), which is a valid approximation at high neutrino energies; integrate over angle; and use Eq. (A35) to get the expressions given in Bruenn [9] (with N and Z interchanged), viz.,

$$\Phi_{0\nu-A}^{\text{high}} - \Phi_{1\nu-A}^{\text{high}} = \frac{2\pi}{\hbar} n_{\text{nuc}} \frac{G^2}{V} A^2 \left| C_{V0} + C_{V1} \frac{Z-N}{2A} \right|^2 \left[\frac{2y-1+e^{-2y}}{y^2} - \frac{2-3y+2y^2-(2+y)e^{-2y}}{y^3} \right], \quad (\text{A49})$$

where

$$y = 4b \frac{E_\nu^2}{c^2} = \frac{2}{3} \frac{^{3/5}(1.07A)^{2/3} E_\nu^2}{(\hbar c)^2}. \quad (\text{A50})$$

Here the superscript ‘‘high’’ is a reminder that this expression for $\Phi_{0\nu-A} - \Phi_{1\nu-A}$ is valid only at high neutrino energies.

To obtain an expression for $\Phi_{1\nu-A} - \Phi_{0\nu-A}$ appropriate for any neutrino energy, note that the expression involving y in

the brackets of Eq. (A49) tends to $\frac{4}{3}$ as $y \rightarrow 0$, and is within 10% of $\frac{4}{3}$ when $y=0.1$, i.e., when $E_\nu = 24.1/A_{56}^{2/3}$ MeV, where $A_{56} = A/56$. Thus, for $E_\nu < 24.1/A_{56}^{2/3}$, Eq. (A49) for $\Phi_{0\nu-A} - \Phi_{1\nu-A}$ is effectively the same as its corresponding expression for low neutrino energies, Eq. (A48), without the ion screening correction $\langle \mathcal{S}_{\text{ion}} \rangle$. Moreover, according to Fig. 2, for $\rho < 10^{13}$ g cm $^{-3}$ the screening correction $\langle \mathcal{S}_{\text{ion}} \rangle$ is close to unity for $E_\nu \gtrsim 24.1/A_{56}^{2/3}$. Therefore a good approximation for $\Phi_{0\nu-A} - \Phi_{1\nu-A}$ at all neutrino energies would simply be given by Eq. (A49) multiplied by $\langle \mathcal{S}_{\text{ion}} \rangle$, i.e.,

$$\Phi_{0\nu-A} - \Phi_{1\nu-A} = \frac{2\pi}{\hbar} n_{\text{nuc}} \frac{G^2}{V} A^2 \left| C_{V0} + C_{V1} \frac{Z-N}{2A} \right|^2 \times \left[\frac{2y-1+e^{-2y}}{y^2} - \frac{2-3y+2y^2-(2+y)e^{-2y}}{y^3} \right] \langle \mathcal{S}_{\text{ion}} \rangle. \quad (\text{A51})$$

This is the expression used for neutrino-nucleus isoenergetic scattering in our supernova code.

-
- [1] H. A. Bethe, *Rev. Mod. Phys.* **62**, 801 (1990).
[2] S. W. Bruenn, in *Nuclear Physics in the Universe*, edited by M. W. Guidry and M. R. Strayer (Institute of Physics and Physical Society, Bristol, 1993), p. 31.
[3] M. E. Herant, W. Benz, W. R. Hix, C. Fryer, and S. A. Colgate, *Astrophys. J.* **435**, 339 (1994).
[4] A. Burrows, J. Hayes, and B. A. Fryxell, *Astrophys. J.* **450**, 830 (1995).
[5] H.-T. Janka and E. Müller, *Astron. Astrophys.* **306**, 167 (1996).
[6] A. Mezzacappa, A. C. Calder, S. W. Bruenn, J. M. Blondin, M. W. Guidry, M. R. Strayer, and A. S. Umar, *Astrophys. J.* (to be published).
[7] A. Yahil, *Astrophys. J.* **265**, 1047 (1983).
[8] S. E. Woosley and T. A. Weaver, *Annu. Rev. Astron. Astrophys.* **24**, 205 (1986).
[9] S. W. Bruenn, *Astrophys. J., Suppl. Ser.* **58**, 771 (1985).
[10] D. L. Tubbs and D. N. Schramm, *Astrophys. J.* **201**, 467 (1975).
[11] H. A. Bethe, J. Applegate, and G. E. Brown, *Astrophys. J.* **241**, 343 (1980).
[12] R. Bowers and J. R. Wilson, *Astrophys. J.* **263**, 366 (1982).
[13] K. Sato, *Prog. Theor. Phys.* **53**, 595 (1975).
[14] K. Sato, *Prog. Theor. Phys.* **54**, 1325 (1975).
[15] T. J. Mazurek, *Astrophys. Space Sci.* **35**, 117 (1975).
[16] T. J. Mazurek, *Astrophys. J., Lett. Ed.* **207**, L87 (1976).
[17] H. A. Bethe, G. E. Brown, J. Applegate, and J. M. Lattimer, *Nucl. Phys.* **A324**, 487 (1979).
[18] D. Z. Freedman, *Phys. Rev. D* **9**, 1389 (1974).
[19] W. R. Yueh and J. R. Buchler, *Astrophys. J.* **217**, 565 (1977).
[20] D. Z. Freedman, D. N. Schramm, and D. L. Tubbs, *Annu. Rev. Nucl. Sci.* **27**, 167 (1977).
[21] N. Itoh, *Prog. Theor. Phys.* **54**, 1580 (1975).
[22] J. P. Hansen, *Phys. Rev. A* **8**, 3096 (1973).
[23] H. Ichimaru, H. Iyetomi, and S. Tanaka, *Phys. Rep.* **149**, 91 (1987).
[24] S. W. Bruenn, *Astrophys. J., Suppl. Ser.* **62**, 331 (1986).
[25] C. Horowitz, *Phys. Rev. D* **55**, 4577 (1997).
[26] S. W. Bruenn and W. C. Haxton, *Astrophys. J.* **376**, 678 (1991).
[27] J. M. Lattimer and F. D. Swesty, *Nucl. Phys.* **A535**, 331 (1991).
[28] F.-K. Thielemann, K. Nomoto, and M. Hashimoto, *Astrophys. J.* **460**, 408 (1996).
[29] J. Cooperstein, *Nucl. Phys.* **A438**, 722 (1985).
[30] E. Baron, J. Cooperstein, and S. Kahana, *Nucl. Phys.* **A440**, 744 (1985).
[31] E. Baron, J. Cooperstein, and S. Kahana, *Phys. Rev. Lett.* **55**, 126 (1985).
[32] S. E. Woosley (private communication).
[33] S. A. Colgate and R. H. White, *Astrophys. J.* **143**, 626 (1966).
[34] W. D. Arnett, *Astrophys. J.* **237**, 541 (1980).
[35] R. I. Epstein and C. J. Pethick, *Astrophys. J.* **243**, 1003 (1981).
[36] K. A. Van Riper and J. M. Lattimer, *Astrophys. J.* **249**, 270 (1981).
[37] S. A. Bludman, I. Lichtenstadt, and G. Hayden, *Astrophys. J.* **261**, 661 (1982).
[38] S. W. Bruenn (unpublished).
[39] G. E. Brown, H. A. Bethe, and G. Baym, *Nucl. Phys.* **A375**, 481 (1982).
[40] E. R. Cohen and B. N. Taylor, *Rev. Mod. Phys.* **59**, 1121 (1987).
[41] E. D. Commins and P. W. Bucksbaum, *Weak Interactions of Leptons and Quarks* (Cambridge University Press, Cambridge, England, 1983), p. 178.

- [42] S. Weinberg, *Phys. Rev. D* **5**, 1412 (1972).
- [43] F. Seitz, *Modern Theory of Solids* (McGraw-Hill, New York, 1940), p. 470.
- [44] *Nuclear and Nucleon Structure*, edited by R. Hofstadter (Benjamin, New York, 1963).
- [45] Léon Van Hove, *Phys. Rev.* **95**, 249 (1954).
- [46] D. Pines and P. Nozières, *The Theory of Quantum Liquids, Volume I: Normal Fermi Liquids* (Benjamin, New York, 1966).
- [47] J. P. Hansen and I. R. McDonald, *Theory of Simple Liquids* (Academic, New York, 1976).